

Peak Estimation of Time Delay Systems using Occupation Measures

Jared Miller¹, Milan Korda^{2,3}, Victor Magron^{2,4}, Mario Sznaier¹

April 6, 2023

Abstract

This work proposes a method to compute the maximum value obtained by a state function along trajectories of a Delay Differential Equation (DDE). An example of this task is finding the maximum number of infected people in an epidemic model with a nonzero incubation period. The variables of this peak estimation problem include the stopping time and the original history (restricted to a class of admissible histories). The original nonconvex DDE peak estimation problem is approximated by an infinite-dimensional Linear Program (LP) in occupation measures, inspired by existing measure-based methods in peak estimation and optimal control. This LP is approximated from above by a sequence of Semidefinite Programs (SDPs) through the moment-Sum of Squares (SOS) hierarchy. Effectiveness of this scheme in providing peak estimates for DDEs is demonstrated with provided examples.

1 Introduction

This paper presents an algorithm to upper bound extreme values of a state function attained along trajectories of a Delay Differential Equation (DDE). The dynamics of a DDE depend on a history of the state, in contrast to an Ordinary Differential Equation (ODE) in which the dynamics are a function only of the present values of state [1, 2, 3, 4]. This paper will involve analysis of DDEs in a state space $X \subset \mathbb{R}^n$ over a time horizon $T < \infty$ with a single fixed discrete bounded delay $\tau \in (0, T)$.

Trajectory evolution of a DDE depends on an initial history $x_h : [-\tau, 0] \rightarrow X$ rather than simply an initial condition $x_0 \in X$ for a corresponding ODE. The evaluation at time t for a trajectory starting with a history x_h will be denoted as $x(t | x_h)$. A function class \mathcal{H} of histories may be defined, allowing for the definition of differential inclusions of DDEs. A peak estimation problem may be defined on a time-delay system to find the maximum value of a state function p along system trajectories given a class of initial histories \mathcal{H} as

$$P^* = \sup_{t^* \in [0, T], x_h(\cdot)} p(x(t^* | x_h)) \quad (1a)$$

$$\dot{x} = f(t, x(t), x(t - \tau)) \quad \forall t \in [0, T] \quad (1b)$$

$$x(t) = x_h(t) \quad \forall t \in [-\tau, 0] \quad (1c)$$

$$x_h(\cdot) \in \mathcal{H}. \quad (1d)$$

¹J. Miller, and M. Sznaier are with the Robust Systems Lab, ECE Department, Northeastern University, Boston, MA 02115. (e-mails: miller.jare@northeastern.edu, msznaier@coe.neu.edu).

²Polynomial OPTimization Team, LAAS-CNRS, Toulouse, 31400, France

³Faculty of Electrical Engineering, Czech Technical University in Prague, Technická 2, CZ-16626 Prague, Czech Republic

⁴Institut de Mathématiques de Toulouse, 31062, France

J. Miller and M. Sznaier were partially supported by NSF grants ECCS-1808381 and CNS-2038493, AFOSR grant FA9550-19-1-0005, and ONR grant N00014-21-1-2431. J. Miller was in part supported by the Chateaubriand Fellowship (performed at LAAS-CNRS) of the Office for Science & Technology of the Embassy of France in the United States, and by the International Student Exchange Program from AFOSR.

The work of M. Korda and V. Magron was partly supported by the European Union's Horizon 2020 research and innovation programme under the Marie Skłodowska-Curie Actions, grant agreement 813211 (POEMA). The work of M. Korda was also partly supported by the Czech Science Foundation (GACR) under contract No. 20-11626Y, and by the AI Interdisciplinary Institute (ANITI) funding, through the French "Investing for the Future PIA3" program under the Grant agreement ANR-19-P13A-0004.

The variables in Problem (1) are the stopping time t^* and the initial history x_h . Problem (1) is a DDE version of the (generically nonconvex) ODE peak estimation program studied in [5, 6]. The peak estimation task in (1) is an instance of a DDE Optimal Control Problem (OCP) with a free terminal time and a zero running (integrated) cost.

This work uses measure-theoretic methods in order to provide certifiable upper bounds on the peak value P^* from (1). The first application of measure-theoretic methods towards DDEs was in [7], in which the control input was relaxed into a Young Measure [8] (probability distribution at each point in time) [9]. This Young-Measure-based relaxed control yields the OCP optimal value in the case of a single discrete time delay under convexity, regularity, and compactness assumptions. However, the Young Measure control programs may result in a lower bound when there are two or more delays in the system dynamics (there exist Young-Measure solutions that do not correspond to OCP solutions) [10, 11]. Adding new measures and constraints allows for the construction of tight Young Measure OCP approximations at the cost of significantly more complicated programs [12].

Occupation measures are nonnegative Borel measures that contain all possible information about trajectory behavior, and are a step beyond Young Measures in terms of abstraction and relaxation. The work of [13] proves that a convex infinite-dimensional Linear Program (LP) in occupation measures for an ODE OCP has the same optimal value as the original OCP under compactness, convexity, and regularity conditions. The problem of estimation of the peak of the expected value of a given state function for stochastic processes may be solved using occupation measures under these same conditions [5]. The Moment-Sum of Squares (SOS) hierarchy offers a sequence of outer approximations (lower bounds on OCP/upper bounds on peak estimates) as found through solving Semidefinite Programs (SDPs) of increasing size [14]. The moment-SOS hierarchy has been applied to dynamical problems including barrier functions [15], OCPs [16, 17], peak estimation [6, 18], region of attraction estimation [19], reachable set estimation [20] and distance estimation [21].

Use of the moment-SOS hierarchy towards analysis of DDEs includes finding stability and safety certificates [22, 23, 17]. Prior work on using occupation measures for problems in time delays includes ODE-PDE models in [24, 25], a Riesz-frame system in [26], and a gridded LP framework for optimal control given a single history x_h in [27]. Peak estimation has been conducted on specific time-delay systems such as the forced Liénard model [28] and compartmental epidemic models [29].

The contributions of this paper are:

- A theory of Measure-Valued (MV)-solutions to DDEs with multiple histories (in \mathcal{H}) and free terminal time
- A measure LP that upper-bounds problem (1)
- A convergent sequence of Linear Matrix Inequalities (LMIs) (and resultant SDPs) to the measure upper-bound

This paper is organized as follows: Section 2 formalizes notation and summarizes concepts in measure theory, time-delay, occupation measures, and ODE peak estimation. Section 3 defines MV-solutions for free-terminal-time DDE trajectories to create a primal-dual pair of LPs to upper-bound (1). Section 4 applies the Moment-SOS hierarchy towards generating SDPs to upper-bound the peak-estimation measure LP. Section 5 provides examples of DDE peak estimation. Section 6 extends the DDEs peak framework by allowing for distance estimation, shaping constraints on histories, and uncertainty. Section 7 concludes the paper. Appendix A extends the MV-solution framework towards continuous-time systems with proportional delays and discrete-time systems with long time delays. Appendix B performs the proof of strong duality for the DDEs peak estimation LPs. Appendix C finds and analyzes structural properties of DDE OCPs subvalue functionals. Appendix D reduces conservatism of OCP approximations by performing spatio-temporal partitioning and applying double-integral subvalue functionals. Appendix E introduces a more conservative but computationally simpler notion of MV-solution for DDEs.

2 Preliminaries

2.1 Notation

The n -dimensional real Euclidean vector space is \mathbb{R}^n . The set of natural numbers is \mathbb{N} , and the set of n -dimensional multi-indices is \mathbb{N}^n . The degree of a multi-index $\alpha \in \mathbb{N}^n$ is $|\alpha| = \sum_{i=1}^n \alpha_i$. The set of polynomials with real coefficients in an indeterminate x is $\mathbb{R}[x]$. Each polynomial $p(x) \in \mathbb{R}[x]$ has a unique representation in terms of a finite index set $\mathcal{J} \subset \mathbb{N}^n$ and coefficients $\{p_\alpha\}_{\alpha \in \mathcal{J}}$ with $p_\alpha \neq 0$ as $p(x) = \sum_{\alpha \in \mathcal{J}} p_\alpha (\prod_{i=1}^n x_i^{\alpha_i}) = \sum_{\alpha \in \mathcal{J}} p_\alpha x^\alpha$. The degree of a polynomial $\deg p(x)$ is equal to $\max_{\alpha \in \mathcal{J}} |\alpha_j|$. The subset of polynomials with degree at most d is $\mathbb{R}[x]_{\leq d} \subset \mathbb{R}[x]$.

2.2 Analysis and Measure Theory

Let X be a topological space. The set of continuous functions over a space X is $C(X)$, and its subcone of nonnegative functions over X is $C_+(X)$. The subset of once-differentiable functions over X is $C^1(X) \subset C(X)$. A single-variable function $g(t)$ is Piecewise Continuous (PC) over the domain $[a, b]$ if there exist $B \in \mathbb{N} \setminus \{0\}$ and a finite number of time-breaks $t_0 = a < t_1 < t_2 < \dots < t_B < b = t_{B+1}$ such that the function $g(t)$ is continuous in each interval $[t_k, t_{k+1})$ for $k = 0..B$. The class of PC functions from the time interval $[-\tau, 0]$ to X is $PC([-\tau, 0], X)$.

The set of nonnegative Borel measures over X is $\mathcal{M}_+(X)$. A pairing exists between functions $p \in C(X)$ and measures $\mu \in \mathcal{M}_+(X)$ by Lebesgue integration with $\langle p, \mu \rangle = \int_X p(x) d\mu(x)$. This pairing is a duality pairing and defines an inner product between $C_+(X)$ and $\mathcal{M}_+(X)$ when X is compact. The μ -measure of a set $A \subseteq X$ may be defined in terms of A 's indicator function ($I_A(x) = 1$ if $x \in A$ and $I_A(x) = 0$ otherwise) as $\mu(A) = \langle I_A(x), \mu(x) \rangle$. The quantity $\mu(X)$ is called the mass of μ , and μ is a probability distribution if $\mu(X) = 1$. The support of μ is the set of all points x such that all open neighborhoods $N_x \ni x$ satisfy $\mu(N_x) > 0$. Two special measures are the Dirac delta and the Lebesgue measure. The Dirac delta δ_x with respect to a point $x \in X$ obeys the point-evaluation pairing $\langle p, \delta_x \rangle = p(x)$ for all $p \in C(X)$. The Lebesgue (volume) distribution has the definition $\langle p, \lambda_X \rangle = \int_X p(x) dx$. Further details about measure theory are available in [30].

Given spaces X and Y , the projection $\pi^x : X \times Y \rightarrow X$ is the map $(x, y) \mapsto x$. For measures $\mu \in \mathcal{M}_+(X)$ and $\nu \in \mathcal{M}_+(Y)$, the product measure $\mu \otimes \nu \in \mathcal{M}_+(X \times Y)$ is the unique measure satisfying $(\mu \otimes \nu)(A \times B) = \mu(A)\nu(B)$ for all subsets $A \subseteq X$, $B \subseteq Y$. For two measures $\mu, \xi \in \mathcal{M}_+(X)$, the measure μ dominates ξ ($\xi \leq \mu$) if $\xi(A) \leq \mu(A)$, $\forall A \subset X$. To every dominated measure $\xi \leq \mu$, there exists a slack measure $\hat{\xi} \in \mathcal{M}_+(X)$ such that $\xi + \hat{\xi} = \mu$.

The pushforward of a map $Q : X \rightarrow Y$ along a measure μ is $Q_{\#}\mu$, with the relation $\langle z, Q_{\#}\mu \rangle = \langle z \circ Q, \mu \rangle$ holding for all $z \in C(Y)$. Given $\eta \in \mathcal{M}_+(X \times Y)$, the projection-pushforward $\pi_{\#}^x \eta$ is the x -marginalization of η . The pairing of $p \in C(X)$ with $\pi_{\#}^x \eta$ may be equivalently expressed as $\langle p, \pi_{\#}^x \eta \rangle = \langle p, \eta \rangle$. The adjoint of a linear map $\mathcal{L} : C(X) \rightarrow C(Y)$ is a mapping $\mathcal{L}^\dagger : M(Y) \rightarrow M(X)$ satisfying $\langle \mathcal{L}p, \nu \rangle = \langle p, \mathcal{L}^\dagger \nu \rangle$ for all $p \in C(X)$ and $\nu \in M(Y)$.

2.3 Time Delay Systems

A single-variable function $g(t)$ is PC over the domain $[a, b]$ if there exist $B \in \mathbb{N} \setminus \{0\}$ and a finite number of time-breaks $t_0 = a < t_1 < t_2 < \dots < t_B < b = t_{B+1}$ such that the function $g(t)$ is continuous in each interval $[t_k, t_{k+1})$ for $k = 0..B$. The class of PC functions from the time interval $[-\tau, 0]$ to X is $PC([-\tau, 0], X)$.

Given a PC state history $t \mapsto x_h(t)$, $t \in [-\tau, 0]$, a unique forward trajectory $x(t | x_h)$ of (1b) exists on $t \in [0, T]$ if the function $(t, x_0, x_1) \mapsto f(t, x_0, x_1)$ is locally Lipschitz in all variables.

Trajectories of time-delay systems with the form of (1b) with f locally Lipschitz satisfy a smoothing property as shown in Figure 1. The order of derivatives that are continuous will increase by 1 every τ time steps [4]. An example of such a time-delay system with increasing continuity is visualized in Figure 1 with system dynamics

$$x'(t) = -2x(t) - 2x(t-1). \quad (2)$$

Figure 2 plots multiple trajectories of (2) whose histories are lines passing through $x_h(0) = 1$, but whose evolution after time $t = 0$ is different.

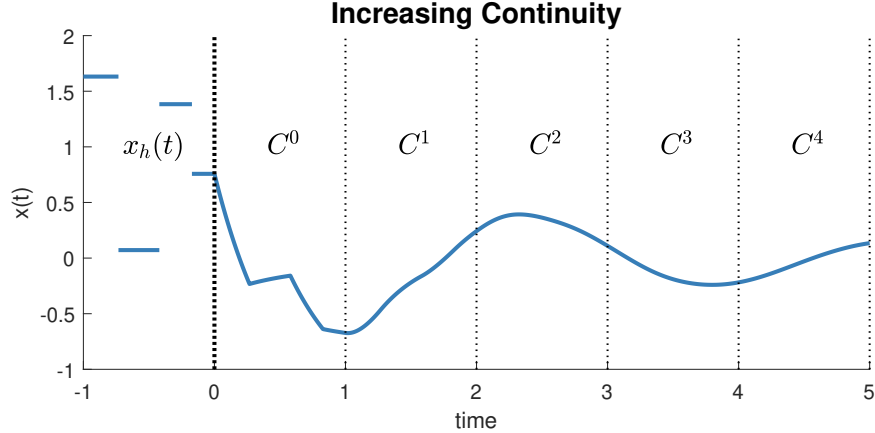


Figure 1: Continuity of (2) trajectories increases every $\tau = 1$ time step

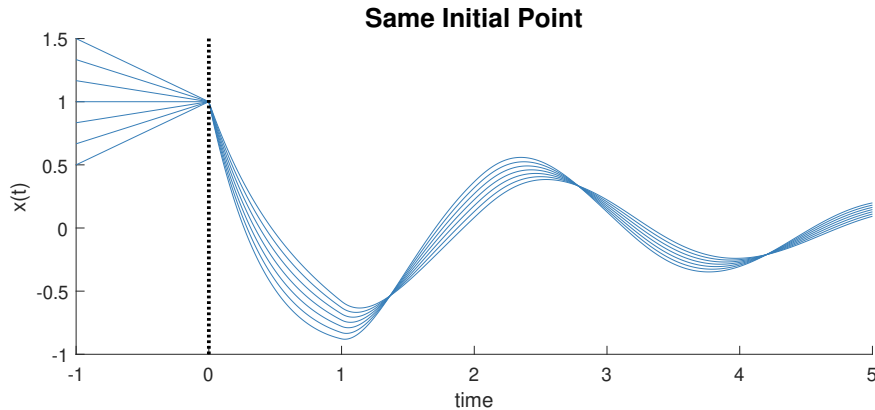


Figure 2: All histories of Figure (2) pass through $x_h(0) = 1$

The behavior of time-delay systems may change and bifurcate as the time delays change. A well-studied example of $\dot{x} = -x(t - \tau)$ is plotted in Figure (3) [4], in which the system is stable (to $x = 0$) for all bounded PC histories with $\tau \in [0, \pi/2)$, has bounded oscillations for some initial histories at $\tau = \pi/2$ (e.g., constant x_h in time), and is unstable (divergent oscillations to $\pm\infty$) for all similar histories with $\tau > \pi/2$ [4].

Problem (1) involves a class of histories \mathcal{H} . In this paper, we will impose that \mathcal{H} is graph-constrained:

Definition 2.1. *The history class \mathcal{H} is **graph-constrained** if \mathcal{H} is the set of histories whose graph lies within a given set $H_0 \subseteq [-\tau, 0] \times X$,*

$$\mathcal{H} = \{x_h \in PC([-\tau, 0], X) \mid (t, x_h(t)) \in H_0 \forall t \in [-\tau, 0]\},$$

and there are no other continuity restrictions on histories.

2.4 Occupation Measures

The **occupation measure** associated with an interval $[a, b] \subset \mathbb{R}$ and a curve $t \mapsto x(t) \in PC([a, b], X)$ is the pushforward of the Lebesgue distribution (in time) $\lambda_{[a, b]}$ along the curve evaluation. Such an occupation measure $\mu_{x(\cdot)} \in \mathcal{M}_+([a, b] \times X)$ satisfies a relation for all $v \in C([a, b] \times X)$:

$$\langle v, \mu_{x(\cdot)} \rangle = \int_a^b v(t, x(t)) dt. \quad (3)$$

Occupation measures can be extended to controlled dynamics. Let $U \subset \mathbb{R}^m$ be a set of input-values and

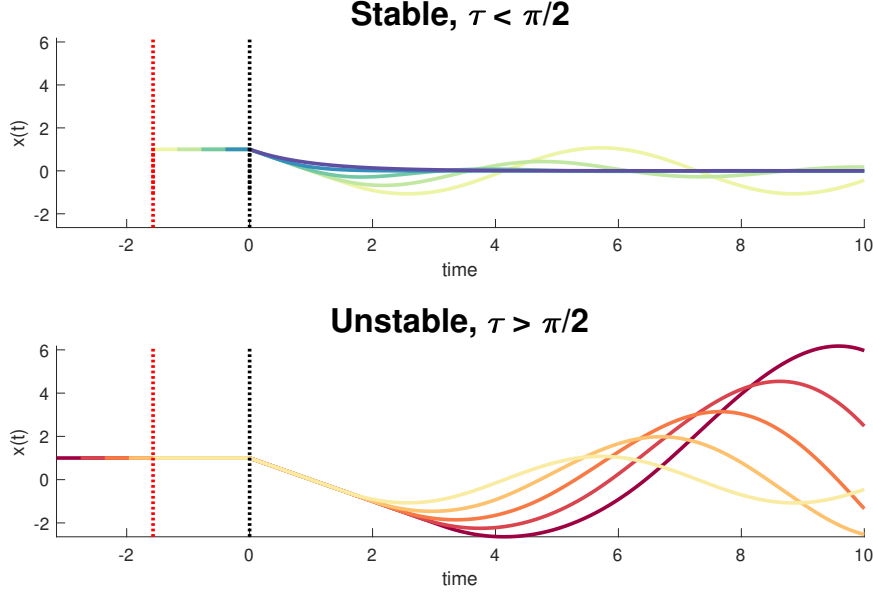


Figure 3: Bifurcation of stability as τ exceeds $\pi/2$ in $\dot{x} = -x(t - \tau)$

define the following controlled dynamics (in which $u(t) \in U$ for all $t \in [0, T]$) :

$$\dot{x}(t) = f(t, x(t), u(t)). \quad (4)$$

The occupation measure of a trajectory of (4) given a stopping time t^* , an initial condition $x_0 \in X_0 \subset X$ and a measurable control $u(\cdot)$ (such that $u(t)$ is a probability distribution over U for each $t \in [0, t^*]$) for sets $A \subseteq [0, T]$, $B \subseteq X$, $C \subseteq U$, is

$$\begin{aligned} \mu(A \times B \times C \mid t^*, x_0) = \\ \int_{[0, t^*] \times X_0 \times U} I_{A \times B \times C}((t, x(t) \mid x_0, u(\cdot)), u(t)) dt. \end{aligned} \quad (5)$$

The occupation measure in (5) may be averaged over a distribution of initial conditions $\mu_0(x_0)$:

$$\begin{aligned} \mu(A \times B \times C \mid t^*) = \\ \int_{X_0} \mu(A \times B \times C \mid t^*, x_0) d\mu_0(x_0). \end{aligned} \quad (6)$$

A linear operator \mathcal{L}_f may be defined for every $v \in C^1([-\tau, T] \times \mathbb{R}^n)$ by

$$\mathcal{L}_f v(t, x) = \partial_t v(t, x) + f(t, x, u) \cdot \nabla_x v(t, x). \quad (7)$$

A distribution of initial conditions $\mu_0 \in \mathcal{M}_+(X_0)$, free-terminal-time values $\mu_p \in \mathcal{M}_+([0, T] \times X)$, and occupation measures $\mu \in \mathcal{M}_+([0, T] \times X \times U)$ from (6) are connected together by Liouville's equation for all $v \in C^1([0, T] \times X)$:

$$\langle v, \mu_p \rangle = \langle v(0, x), \mu_0(x) \rangle + \langle \mathcal{L}_f v, \mu \rangle \quad (8a)$$

$$\mu_p = \delta_0 \otimes \mu_0 + \pi_{\#}^{tx} \mathcal{L}_f^\dagger \mu. \quad (8b)$$

Equation (8b) is a shorthand notation for (8a) when applied to all C^1 functions v . Note that the $\pi_{\#}^{tx}$ marginalizes out the input u in the occupation measure μ . Any μ as part of a tuple of measures (μ_0, μ_p, μ) satisfying (8) is referred to as a **relaxed occupation measure**.

3 Peak Measure Program

This section will formulate a measure-valued LP which upper-bounds Problem (1) in objective.

3.1 Assumptions

The following assumptions will be imposed on the peak estimation Problem (1):

- A1 The set $[-\tau, T] \times X$ is compact with $\tau < T$;
- A2 The function f is Lipschitz inside $[0, T] \times X^2$;
- A3 Any trajectory $x(\cdot | x_h)$ with $x_h \in \mathcal{H}$ such that $x(t | x_h) \notin X$ for some $t \in [0, T]$ also satisfies $x(t' | x_h) \notin X$ for all $t' \geq t$;
- A4 The objective p is continuous;
- A5 The history class \mathcal{H} is graph-constrained by $H_0 \subset [-\tau, 0] \times X$.

In the case where $\tau > T$, the delayed state $t \mapsto x(t - \tau)$ is fully specified in time $[0, T]$ without requiring dynamics information, and (1) reduces to a peak estimation problem over ODEs. All tracked histories in \mathcal{H} are bounded due to assumption A1 (since the range X is compact). The nonreturn assumption A3 ensures that a trajectory cannot leave and then return to X to produce a lower value of p , given that the occupation-measure-based techniques used in this paper can only track trajectories while they are in X .

3.2 Measure-Valued Solution

The initial set X_0 is the $t = 0^+$ slice of H_0 . Equation (9) describes the measures $(\mu_h, \mu_0, \mu_p, \bar{\mu}_0, \bar{\mu}_1, \nu)$ that will be used to form a free-terminal-time MV-solution to the DDE (1b) with multiple histories (in \mathcal{H}):

History	$\mu_h \in \mathcal{M}_+(H_0)$	(9a)
Initial	$\mu_0 \in \mathcal{M}_+(X_0)$	(9b)
Peak	$\mu_p \in \mathcal{M}_+([0, T] \times X)$	(9c)
Occupation Start	$\bar{\mu}_0 \in \mathcal{M}_+([0, T - \tau] \times X^2)$	(9d)
Occupation End	$\bar{\mu}_1 \in \mathcal{M}_+([T - \tau, T] \times X^2)$	(9e)
Time-Slack	$\nu \in \mathcal{M}_+([0, T] \times X)$	(9f)

The joint (relaxed) occupation measure $\bar{\mu} \in \mathcal{M}_+([0, T] \times X^2)$ is constructed from the sum $\bar{\mu} = \bar{\mu}_0 + \bar{\mu}_1$. An MV solution to the DDE in (1b) is a set of measures from (9) that satisfy three types of constraints: History-Validity, Liouville, Consistency.

3.2.1 History-Validity

The first History-Validity constraint is that μ_0 should be a probability distribution over the initial state condition (at $t = 0$). The second is that the history measure μ_h should represent an averaged occupation measure of histories that are defined between $[-\tau, 0]$, which implies that the t -marginal of μ_h should be Lebesgue-distributed. The two History-Validity constraints are,

$$\langle 1, \mu_0 \rangle = 1, \quad \pi_{\#}^t \mu_h = \lambda_{[-\tau, 0]}. \quad (10)$$

3.2.2 Liouville

The true occupation measure $(t, x_0, x_1) \mapsto \bar{\mu}(t, x_0, x_1)$ has a time t , a current state $x_0 = x(t | x_h)$, and an external input $x_1 \in X$ with $x_1(t) = x(t - \tau | x_h)$. Use of the Liouville equation in (8) applied to the joint occupation measure $\bar{\mu} = \bar{\mu}_0 + \bar{\mu}_1$ leads to

$$\mu_p = \delta_0 \otimes \mu_0 + \pi_{\#}^{tx_0} \mathcal{L}_f^\dagger(\bar{\mu}_0 + \bar{\mu}_1). \quad (11)$$

3.2.3 Consistency

The x_1 input of f from the Liouville equation (11) is not arbitrary; it should be equal to a time-delayed $x_1(t) = x_0(t - \tau)$. This requirement will be imposed by a Consistency constraint.

Lemma 3.1. *Let $x(\cdot)$ be a solution to (1b) for some history x_h with an initial time of 0 and a stopping time of $t^* \in [0, T]$. Then the following two integrals are equal for all $\phi \in C([0, T] \times X)$:*

$$\begin{aligned} & \left(\int_0^{t^*} + \int_{t^*}^{\min(T, t^* + \tau)} \right) \phi(t, x(t - \tau)) dt \\ &= \left(\int_{-\tau}^0 + \int_0^{\min(t^*, T - \tau)} \right) \phi(t' + \tau, x(t)) dt'. \end{aligned} \quad (12)$$

Proof. This follows from a change of variable with $t' \leftarrow t - \tau$. \square

Equation (12) inspires a consistency constraint for the free-terminal-time MV-solution in (9). The left-hand-side of (12) may be generalized to

$$\langle \phi(t, x_1), \bar{\mu}_0(t, x_0, x_1) + \bar{\mu}_1(t, x_0, x_1) \rangle + \langle \phi(t, x), \nu(t, x) \rangle, \quad (13)$$

in which $\bar{\mu}_0$ is supported in times $[0, \min(t^*, T - \tau)]$, $\bar{\mu}_1$ is supported in times $[T - \tau, t^*]$ if $t^* > T - \tau$, and the slack measure ν implements the $[t^*, \min(T, t^* + \tau)]$ limits. The right-hand-side of (12) may be interpreted as

$$\langle \phi(t + \tau, x), \mu_h(t, x) \rangle + \langle \phi(t + \tau, x_0), \bar{\mu}_0(t, x_0, x_1) \rangle. \quad (14)$$

Define S^τ as the shift operator $S^\tau \phi(t, x) = \phi(t + \tau, x)$. With an abuse of notation, the pushforward operation $S_{\#}^\tau$ applied to a measure (such as μ_h) will have the expression

$$\langle \phi, S_{\#}^\tau \mu_h \rangle = \langle S^\tau \phi, \mu_h \rangle = \langle \phi(t + \tau, x), \mu_h(t, x) \rangle. \quad (15)$$

The Consistency constraint inspired by Lemma 3.1 is

$$\pi_{\#}^{tx_1}(\bar{\mu}_0 + \bar{\mu}_1) + \nu = S_{\#}^\tau(\mu_h + \pi_{\#}^{tx_0} \bar{\mu}_0). \quad (16)$$

Remark 1. *Equation (16) may also be written as $\pi_{\#}^{tx_1}(\bar{\mu}_0 + \bar{\mu}_1) \leq S_{\#}^\tau(\mu_h + \pi_{\#}^{tx_0} \bar{\mu}_0)$. The associated slack measure is ν .*

3.3 Measure Program

An infinite-dimensional LP in terms of the measures from (9) to upper-bound Problem (1) is,

$$p^* = \sup \langle p, \mu_p \rangle \quad (17a)$$

$$\langle 1, \mu_0 \rangle = 1 \quad (17b)$$

$$\pi_{\#}^t \mu_h = \lambda_{[-\tau, 0]} \quad (17c)$$

$$\mu_p = \delta_0 \otimes \mu_0 + \pi_{\#}^{tx_0} \mathcal{L}_f^\dagger(\bar{\mu}_0 + \bar{\mu}_1) \quad (17d)$$

$$\pi_{\#}^{tx_1}(\bar{\mu}_0 + \bar{\mu}_1) + \nu = S_{\#}^\tau(\mu_h + \pi_{\#}^{tx_0} \bar{\mu}_0) \quad (17e)$$

$$\text{Measure Definitions from (9)}. \quad (17f)$$

Remark 2. *Membership in the history class \mathcal{H} is imposed by the History-Validity constraint (17c) and through support of μ_h in (9a).*

Definition 3.1. *An MV-solution to the DDE (1b) with free-terminal-time and histories in \mathcal{H} is a tuple of measures that satisfy (17b)-(17f) and (9a)-(9f).*

Theorem 3.2. *Under assumptions A1-A5, (17) will upper bound (1) with $p^* \geq P^*$ when \mathcal{H} is graph-constrained.*

Proof. This proof will proceed by demonstrating that every (t^*, x_h) candidate from (1) may be expressed by a unique MV-solution from Defn. 3.1. The history measure μ_h is the $[-\tau, 0]$ occupation measure of $x(t)$, and the initial measure μ_0 is the Dirac-delta $\delta_{x_h(0^+)}$. The peak measure μ_p is the Dirac-delta $\delta_{t=t^*} \otimes \delta_{x=x(t^*|x_h)}$. The relaxed occupation measures $(\bar{\mu}_0, \bar{\mu}_1, \nu)$ will now be considered. For convenience, define $z(t) = (t, x(t | x_h), x(t - \tau | x_h))$ as the delay embedding of the trajectory $x(t | x_h)$. In the case where $t^* \in [0, T - \tau]$, then $\bar{\mu}_0$ is the $[0, t^*]$ occupation measure of $z(t)$, $\bar{\mu}_1$ is the zero measure, and ν is the $[t^*, t^* + \tau]$ occupation measure of $(t, x(t - \tau | x_h))$. Alternatively when $t^* \in (T - \tau, T]$, $\bar{\mu}_0$ is the $[0, T - \tau]$ occupation measure of $z(t)$, $\bar{\mu}_1$ is the $[T - \tau, t^*]$ occupation measure of $z(t)$, and ν is the $[t^*, T]$ occupation measure of $(t, x(t - \tau | x_h))$. All of the measures in (9) have been defined for each input (t^*, x_h) , which proves that $p^* \geq P^*$. \square

Appendix A uses these methods to form MV-solutions to systems with other delay structures (proportional delay, long-delay discrete-time systems).

Remark 3. The proof of Theorem 3.2 provides a unique MV solution for each DDE trajectory. Additionally, each DDE trajectory given an initial condition x_h is unique under the Lipschitz assumption A2.

We note that MV solutions are not necessarily unique (for a given terminal time distribution $\pi_{\#}^t \mu_p$) when the history measure μ_h is supported on the graph of more than one curve. As an example, Figure 4 shows two sets of curves under the dynamics $\dot{x}(t) = -2x(t) - 3x(t - 1)$ in the times $t \in [0, 5]$. The history occupation measure $\mu_h = 0.5\lambda_{[-1,0]} \otimes \delta_{x=1} + 0.5\lambda_{[-1,0]} \otimes \delta_{x=-1}$ is supported in the set $\mu_h \in \mathcal{M}_+([-1, 0] \times \{-1, 1\})$. The superposition of each set of red and blue curves each have the same history measure μ_h , but the switch that takes place on the bottom plot (e.g. blue: $x_h(t) = 1$ for $t \in [-1, -0.5)$, $x_h(t) = -1$ for $t \in [0.5, 0]$) yields a different trajectory going forward in time.

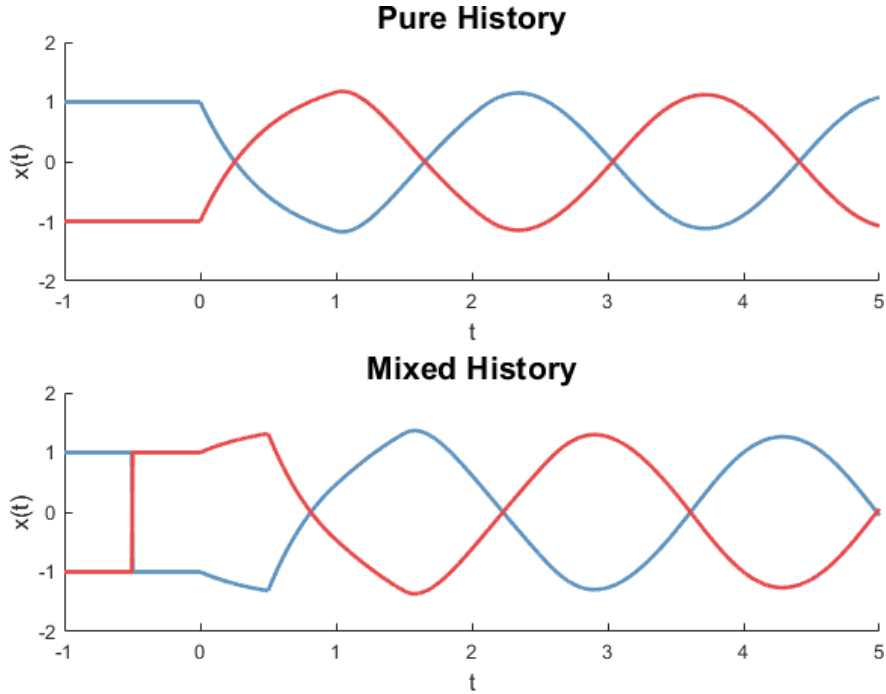


Figure 4: The same μ_h leads to different trajectories in times $(0, 5]$

3.4 Function Program

The dual program of (17) with variables (γ, ξ, v, ϕ) is

$$d^* = \inf_{\gamma \in \mathbb{R}} \gamma + \int_{-\tau}^0 \xi(t) dt \quad (18a)$$

$$\xi(t) + \phi(t + \tau, x) \geq 0 \quad \forall (t, x) \in H_0 \quad (18b)$$

$$\gamma \geq v(0, x) \quad \forall x \in X_0 \quad (18c)$$

$$v(t, x) \geq p(x) \quad \forall (t, x) \in [0, T] \times X \quad (18d)$$

$$\phi(t, x) \leq 0 \quad \forall (t, x) \in [0, T] \times X \quad (18e)$$

$$\mathcal{L}_f v(t, x_0) + \phi(t, x_1) \leq \phi(t + \tau, x_0) \quad \forall (t, x_0, x_1) \in [0, T - \tau] \times X^2 \quad (18f)$$

$$\mathcal{L}_f v(t, x_0) + \phi(t, x_1) \leq 0 \quad \forall (t, x_0, x_1) \in [T - \tau, T] \times X^2 \quad (18g)$$

$$\xi \in C([-\tau, 0]) \quad (18h)$$

$$v \in C^1([0, T] \times X) \quad (18i)$$

$$\phi \in C([0, T] \times X). \quad (18j)$$

Theorem 3.3. *There is no duality gap between (17) and (18).*

Proof. See Appendix B. □

We pose the following conjecture based on [13, 10]:

Conjecture 3.1. *Assume that A1-A5 hold. Additionally, assume that $T > \tau > 0$ and the image-set $f(t, x_0, X)$ is convex for all fixed $t \in [0, T]$, $x_0 \in X$. Then there is no relaxation gap between (1) and (17) ($p^* = P^*$).*

Proving Conjecture 3.1 is the subject of ongoing work.

Appendix C contains a further discussion of the continuity and structural aspects of the dual solution in (18) as applied to bounding costs on DDE OCPs.

4 Peak Moment Program

This section will briefly review the moment-SOS hierarchy [14] in order to approximate-from-above Program (17) by a sequence of finite-dimensional SDPs.

4.1 Review of Moment-SOS Hierarchy

Let $\mu \in \mathcal{M}_+(X)$ be a measure, and let $\alpha \in \mathbb{N}^n$ be a multi-index. The α -moment of μ is the pairing $\mathbf{m}_\alpha = \langle x^\alpha, \mu \rangle$. The moment sequence $\mathbf{m} = \{\mathbf{m}_\alpha\}_{\alpha \in \mathbb{N}^n}$ is the infinite collection of moments of μ . A unique (Riesz) linear functional $L_{\mathbf{m}}$ exists operating on each polynomials $p = \sum_{\alpha \in \mathcal{J}} p_\alpha x^\alpha \in \mathbb{R}[x]$ as $L_{\mathbf{m}}(p) = \sum_{\alpha \in \mathcal{J}} p_\alpha \mathbf{m}_\alpha$ for a finite index set $\mathcal{J} \subset \mathbb{N}^n$.

A set is Basic Semialgebraic (BSA) if it is defined by a finite number of polynomial inequality constraints, such as by $\mathbb{K} = \{x \in \mathbb{R}^n \mid g_k(x) \geq 0 : k = 1 \dots N_c\} \subseteq \mathbb{R}^n$. The measure μ is supported on \mathbb{K} if $\mu \in \mathcal{M}_+(\mathbb{K})$. Given a polynomial $g = \sum_{\gamma \in \mathcal{J}} g_\gamma x^\gamma$, the localizing matrix $\mathbb{M}[g\mathbf{m}]$ induced by the constraint $g(x) \geq 0$ with respect to the moment sequence \mathbf{m} is the infinite-dimensional matrix indexed by $\alpha, \beta \in \mathbb{N}^n$ as $\mathbb{M}[g\mathbf{m}]_{\alpha, \beta} = L_{\mathbf{m}}(x^{\alpha+\beta} g) = \sum_{\gamma \in \mathbb{R}^n} g_\gamma \mathbf{m}_{\alpha+\beta+\gamma}$. The moment matrix $\mathbb{M}[\mathbf{m}]$ is the localizing matrix associated with $g = 1$. The matrix $\mathbb{M}[\mathbb{K}\mathbf{m}]$ is the block-diagonal matrix comprised of $\mathbb{M}[\mathbf{m}]$ and $\mathbb{M}[g_k\mathbf{m}]$ for $k = 1 \dots N_c$.

Let $\{\tilde{\mathbf{m}}_\alpha\}_{\alpha \in \mathbb{N}^n}$ be a sequence of real numbers. If there exists some measure $\tilde{\mu} \in \mathcal{M}_+(\mathbb{K})$ such that $\forall \alpha \in \mathbb{N}^n : \langle x^\alpha, \mu \rangle = \tilde{\mathbf{m}}_\alpha$ then $\tilde{\mu}$ is a representing measure for $\tilde{\mathbf{m}}$, and $\tilde{\mathbf{m}}$ is a moment-sequence for $\tilde{\mu}$. Such a representing measure (if it exists) could be nonunique. The stronger condition that there is a unique representing measure for $\tilde{\mathbf{m}}$ is called moment determinacy. A necessary condition for $\tilde{\mathbf{m}}$ to have a representing measure is that the block-diagonal matrix $\mathbb{M}[\tilde{\mathbf{m}}]$ is Positive Semidefinite (PSD). This necessary condition is also sufficient if \mathbb{K} satisfies an *Archimedean* condition (stronger than compactness, equivalent after a ball

constraint $R - \|x\|_2^2 \geq 0$ is added to \mathbb{K} for sufficiently large $R > 0$ if \mathbb{K} is compact). In general we will call $\tilde{\mathbf{m}}$ a *pseudo-moment* sequence.

The order- d truncation of $\mathbb{M}[\mathbb{K}\mathbf{m}]$ (for $d \in \mathbb{N}$ and expressed as $\mathbb{M}_d[\mathbb{K}\mathbf{m}]$) keeps entries of degree $\leq 2d$, and preserves the top-corner of each matrix in the block-diagonal. The moment matrix $\mathbb{M}_d[\mathbf{m}]$ is a PSD matrix of size $\binom{n+d}{d}$ assuming a monomial basis for x is employed. The size of each truncated localizing matrix $\mathbb{M}_d[g_k\mathbf{m}]$ is $\binom{n+d-\lceil d_k/2 \rceil}{d-\lceil d_k/2 \rceil}$, where $d_k = \deg g_k$. The moment-SOS hierarchy is the process of increasing the degree $d \rightarrow \infty$ when forming moment programs associated to measure LPs.

4.2 Moment Program

Additional assumptions are required in order to approximate (17) using the moment-SOS hierarchy:

A6 The sets H_0 , X_0 , and X are Archimedean BSA sets.

A7 Both p and f are polynomials.

Let the measures $(\mu_h, \mu_0, \mu_p, \bar{\mu}_0, \bar{\mu}_1, \nu)$ have associated pseudo-moment sequences $(\mathbf{m}^h, \mathbf{m}^0, \mathbf{m}^p, \bar{\mathbf{m}}^0, \bar{\mathbf{m}}^1, \mathbf{m}^\nu)$ respectively. Let $\alpha \in \mathbb{N}^n$ and $\beta \in \mathbb{N}$ be multi-indices that define monomial test functions $x_0^\alpha t^\beta$. For each multi-index tuple (α, β) , the operator $\text{Liou}_{\alpha\beta}(\mathbf{m}^0, \mathbf{m}^p, \bar{\mathbf{m}}^0, \bar{\mathbf{m}}^1)$ may be derived from the linear relations induced by the Liouville equation (17d) (in which $\delta_{\beta 0} = 1$ is a Kronecker delta):

$$0 = \langle x^\alpha, \mu_0 \rangle \delta_{\beta 0} + \langle \mathcal{L}(x_0^\alpha t^\beta), \bar{\mu}^0 + \bar{\mu}^1 \rangle - \langle x^\alpha t^\beta, \mu_\tau \rangle. \quad (19)$$

Similarly, the operator $\text{Cons}_{\alpha\beta}(\mathbf{m}^h, \mathbf{m}^\nu, \bar{\mathbf{m}}^0, \bar{\mathbf{m}}^1,)$ may be derived from the consistency constraint (17e) by

$$0 = \langle x_1^\alpha t^\beta, \bar{\mu}^0 + \bar{\mu}^1 \rangle + \langle x^\alpha t^\beta, \nu \rangle - \langle x^\alpha (t + \tau)^\beta, \mu_h \rangle - \langle x_0^\alpha (t + \tau)^\beta, \bar{\mu}^0 \rangle. \quad (20)$$

Given a degree $d \in \mathbb{N}$, the dynamics degree $\tilde{d} \geq d$ may be defined as $\tilde{d} = d + \lfloor \deg f / 2 \rfloor$.

Problem 4.1. Program (17) is upper-bounded by the following order- d LMI in pseudo-moments:

$$p_d^* = \max L_{\mathbf{m}^p}(p) \quad (21a)$$

$$\mathbf{m}_0^0 = 1 \quad (21b)$$

$$\forall (\alpha, \beta) \in \mathbb{N}_{\leq 2d}^{n+1} :$$

$$\mathbf{m}_\beta^h = \int_{-\tau}^0 t^\beta dt = -(-\tau)^{\beta+1} / (\beta + 1) \quad (21c)$$

$$\text{Liou}_{\alpha\beta}(\mathbf{m}^0, \mathbf{m}^p, \bar{\mathbf{m}}^0, \bar{\mathbf{m}}^1) = 0 \quad (21d)$$

$$\text{Cons}_{\alpha\beta}(\mathbf{m}^h, \mathbf{m}^\nu, \bar{\mathbf{m}}^0, \bar{\mathbf{m}}^1,) = 0 \quad (21e)$$

$$\mathbb{M}_d((X_0)\mathbf{m}^0), \mathbb{M}_{\tilde{d}}((H_0)\mathbf{m}^h) \succeq 0 \quad (21f)$$

$$\mathbb{M}_d([0, T] \times X)\mathbf{m}^p \succeq 0 \quad (21g)$$

$$\mathbb{M}_{\tilde{d}}([0, T - \tau] \times X^2)\bar{\mathbf{m}}^0 \succeq 0 \quad (21h)$$

$$\mathbb{M}_{\tilde{d}}([T - \tau, T] \times X^2)\bar{\mathbf{m}}^1 \succeq 0 \quad (21i)$$

$$\mathbb{M}_{\tilde{d}}([0, T] \times X)\mathbf{m}^\nu \succeq 0. \quad (21j)$$

The objective (21a) is the pseudo-moment version of $\langle p, \mu_p \rangle$. Constraints (21c) and (21b) are History-Validity constraints from (10) when applied to the pseudo-moments $(\mathbf{m}^\nu, \mathbf{m}^0)$. Constraints (21d) and (21e) are the Liouville and Consistency constraints respectively. Constraints (21f)-(21j) are support constraints necessary for the pseudo-moments to have representing measures.

Boundedness of all moments of measures in (9) is required to obtain convergence of (21) to (17) as $d \rightarrow \infty$.

Lemma 4.2. All measures from (9) in an MV-solution (Defn. 3.1) are bounded under assumptions A1-A7.

Proof. Boundedness of a measure's mass and support is a sufficient condition that all of the measure's moments are bounded. Assumption A1 ensures compactness, with the requirement from Defn. 2.1 that $H_0 \subseteq [-\tau, X]$ and $X_0 \subseteq X$. The remainder of this proof will involve finding upper bounds on the masses of all measures in (9).

The initial measure μ_0 has a mass of 1, and the history measure μ_h has a mass of τ by the History-Validity constraints (17b) and (17c). Substitution of the test function $v(t, x) = 1$ in the Liouville (17d) leads to $\langle 1, \mu_p \rangle = \langle 1, \mu_0 \rangle = 1$. Since T is finite, the moment $\langle t, \mu_p \rangle \leq \langle 1, \mu_p \rangle (\sup_{t \in [0, T]} t) = T$ is also finite. Use of the test function $v(t, x) = t$ into the Liouville (17d) yields $\langle t, \mu_p \rangle = \langle 1, \bar{\mu}_0 + \bar{\mu}_1 \rangle \leq T$. Because $\bar{\mu}_0$ and $\bar{\mu}_1$ are both nonnegative Borel measures, it holds that $\langle 1, \bar{\mu}_0 \rangle \leq T$ and $\langle 1, \bar{\mu}_1 \rangle \leq T$. The final constraint involves substitution of $\phi(t, x) = 1$ into the Consistency (17e), resulting in

$$\begin{aligned} \langle 1, \bar{\mu}_0 + \bar{\mu}_1 \rangle + \langle 1, \nu \rangle &= \langle 1, \mu_h \rangle + \langle 1, \bar{\mu}_0 \rangle \\ \langle 1, \nu \rangle &= \langle 1, \mu_h \rangle - \langle 1, \bar{\mu}_1 \rangle = \tau - \langle 1, \bar{\mu}_1 \rangle. \end{aligned} \tag{22}$$

Given that $\bar{\mu}_1$ and ν are nonnegative Borel measures and cannot have negative masses, the mass $\langle 1, \nu \rangle$ is constrained within $[0, \tau]$. All masses are demonstrated to be finite, thus proving boundedness. \square

Remark 4. *Neglecting the History-Validity constraint (17c) allows for μ_h in (22) to have infinite mass, violating the boundedness principle.*

Theorem 4.3. *The optima in (21) will converge as $\lim_{d \rightarrow \infty} p_d^* = p^*$ to (17) under assumptions A1-A6.*

Proof. This follows from Corollary 8 of [31] under the boundedness condition in Lemma 4.2. \square

Remark 5. *Assumption A6 can be generalized to cases where the sets (H_0, X_0, X) are the unions of BSA sets. As an example, consider $H_0 = H_0^1 \cup H_0^2$ in which $\pi^t H_0^1 = [-\tau, -\tilde{\tau}]$ and $\pi^t H_0^2 = [-\tilde{\tau}, 0]$ for some $\tilde{\tau} \in (0, \tau)$. Then the pseudo-moments $\mathbf{m}^h = \mathbf{m}_1^h + \mathbf{m}_2^h$ can be implicitly constructed from $\mathbb{M}_d((H_0^1)\mathbf{m}_1^h), \mathbb{M}_d((H_0^2)\mathbf{m}_2^h) \succeq 0$.*

4.3 Computational Complexity

Table 1 lists the size of the order- d PSD moment matrices associated with the pseudo-moment sequences $(\mathbf{m}^h, \mathbf{m}^0, \mathbf{m}^p, \bar{\mathbf{m}}^0, \bar{\mathbf{m}}^1, \mathbf{m}^\nu)$.

Table 1: Size of Moment Matrices in LMI (21)

Matrix:	$\mathbb{M}_d(\mathbf{m}^0)$	$\mathbb{M}_{\bar{d}}(\mathbf{m}^p)$	$\mathbb{M}_d(\mathbf{m}^h)$
Size:	$\binom{n+d}{d}$	$\binom{n+1+d}{d}$	$\binom{n+1+\bar{d}}{\bar{d}}$
Matrix:	$\mathbb{M}_d(\bar{\mathbf{m}}^0)$	$\mathbb{M}_{\bar{d}}(\bar{\mathbf{m}}^1)$	$\mathbb{M}_d(\mathbf{m}^\nu)$
Size:	$\binom{2n+1+d}{\bar{d}}$	$\binom{2n+1+d}{\bar{d}}$	$\binom{n+1+\bar{d}}{\bar{d}}$

The largest size written in Table 1 is $\binom{2n+1+d}{\bar{d}}$, which occurs with the pseudo-moment sequences $(\bar{\mathbf{m}}^0, \bar{\mathbf{m}}^1)$ associated to the two joint occupation measures $(\bar{\mu}_0, \bar{\mu}_1)$. Equality constraints between entries of the moment matrices must be added to convert the LMI into an SDP for use in symmetric-cone Interior Point Methods. The per-iteration complexity of solving an SDP derived from an order- d LMI involved in the moment-SOS hierarchy scales as $O(n^{6d})$ [14] with n . In the case of LMI (21), the computational complexity of solving (21) will scale approximately as $(2n+1)^{6\bar{d}}$ (based on $\bar{\mathbf{m}}^0, \bar{\mathbf{m}}^1$).

4.4 Distance Estimation

The distance estimation framework of [21] may also be applied towards DDEs. The DDE distance estimation program with an unsafe set $X_u \subset X$, a metric $c(x, y)$, and point-unsafe-set distance function $c(x; X_u) =$

$\inf_{y \in X_u} c(x, y)$ is

$$P^* = \inf_{t^* \in [0, T], x_h(\cdot)} c(x(t^* | x_h); X_u) \quad (23a)$$

$$\dot{x} = f(t, x(t), x(t - \tau)) \quad \forall t \in [0, T] \quad (23b)$$

$$x(t) = x_h(t) \quad \forall t \in [-\tau, 0] \quad (23c)$$

$$x_h(\cdot) \in \mathcal{H}. \quad (23d)$$

Safety in program (23) is measured pointwise: a trajectory is safe if $x(t | x_h) \notin X_u$ for every time $t \in [0, T]$. Safety ensuring that the entire history is never contained within X_u ($\exists s \in [-\tau, 0] | x(t - s | x_h) \notin X_u \forall t \in [0, T]$) is a more challenging separate problem and will not be considered here.

The MV-solution in (9) may be applied to (23) to create a DDE distance estimation program by adding a joint probability measure $\eta \in \mathcal{M}_+(X \times X_u)$ (following the procedure from [21]):

$$c^* = \inf \langle c, \eta \rangle \quad (24a)$$

$$\pi_{\#}^x \mu^p = \pi_{\#}^x \eta \quad (24b)$$

$$\langle 1, \mu_0 \rangle = 1 \quad (24c)$$

$$\pi_{\#}^t \mu_h = \lambda_{[-\tau, 0]} \quad (24d)$$

$$\mu_p = \delta_0 \otimes \mu_0 + \pi_{\#}^{tx_0} \mathcal{L}_f^{\dagger}(\bar{\mu}_0 + \bar{\mu}_1) \quad (24e)$$

$$\pi_{\#}^{tx_1}(\bar{\mu}_0 + \bar{\mu}_1) + \nu = S_{\#}^{\tau}(\mu_h + \pi_{\#}^{tx_0} \bar{\mu}_0) \quad (24f)$$

$$\eta \in \mathcal{M}_+(X \times X_u) \quad (24g)$$

$$\text{Measure Definitions from (9)}. \quad (24h)$$

The distance estimation program only affects the cost (24a). This change is orthogonal to the modification in dynamics necessary to create a DDE MV-solution from the ODE program.

5 Numerical Examples

All experiments were developed in MATLAB 2021a, and code is available at <https://github.com/Jarmill/timedelay>. Dependencies include Gloptipoly [32], YALMIP [33], and Mosek [34] in order to formulate and solve moment-SOS LMIs and SDPs.

In this section, a notational convention where (x_1, x_2) correspond to coordinates of $x \in X$ will be used. All sampled histories in visualizations are piecewise-constant inside H_0 with 10 randomly-spaced jumps between $[-\tau, 0]$.

5.1 Epidemic Model

This section provides an example of a MV-solution and peak estimation given a single history in a compartmental epidemic model. Many diseases have incubation periods during which there is a delay between initial infection and infectious potential. In the current COVID-19 pandemic, this incubation period appears to be between 2-14 days, with a median of 5 days [35]. The epidemic dynamics with time delays are

$$S'(t) = -\beta S(t)I(t) \quad (25a)$$

$$I'(t) = \beta S(t - \tau)I(t - \tau) - \gamma I(t) \quad (25b)$$

$$R'(t) = \gamma I(t) \quad (25c)$$

There also exists a 'latent' state $L'(t) = \beta S(t)I(t) - \beta S(t - \tau)I(t - \tau)$ such that $S + I + R + L = 1$. The setting discussed in this section is $\beta = 0.4$, $\gamma = 0.1$, $T = 30$.

Figures 5a and 5b display simulations of this epidemic model as τ changes under a constant state history with $R = 0$. The black curve in Figures 5a and 5b is the plot of $I(t)$ at $\tau = 0$. As the incubation period τ , the time t^* at which the peak is achieved is delayed (moves rightwards) in a monotonically increasing manner. The other colored curves in each plot have delays $\tau \in 1..9$. In Figure 5a with $I_h = 0.1$, the peak

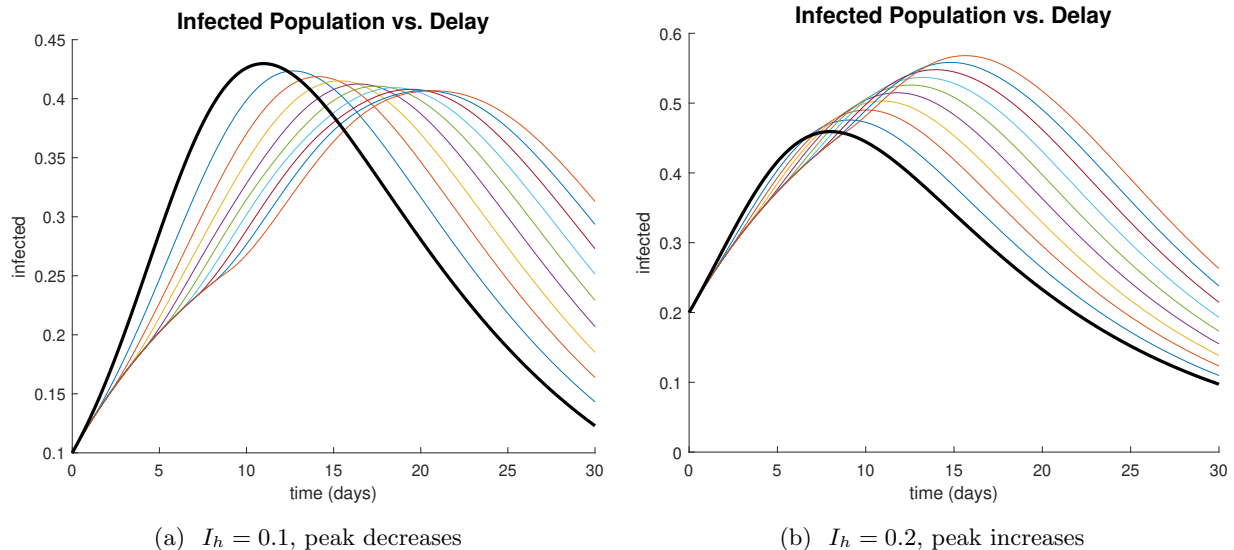


Figure 5: Peak infected population vs. time delay

infected population decreases as the delay τ increases. Conversely in Figure 5b with $I_h = 0.2$, the peak infected population increases as the delay increases.

For the peak estimation example, a constant history is assumed with an initial infection rate of $I_h = 0.2$ and an incubation period of $\tau = 9$, forming the initial history $S(t) = 1 - I_h, I(t) = I_h, R(t) = 0$ between $t \in [-9, 0]$.

For numerical purposes the dynamics are scaled such that $\tilde{t} \in [0, 1]$ with an effective delay of $\tilde{\tau} = \tau/T = 0.3$. Only the $x = (S, I)$ subsystem is considered to form the state set $X = \{S \geq 0, I \geq 0, S + I \leq 1\}$, and the joint occupation measures $(\bar{\mu}_0, \bar{\mu}_1)$ have variables (t, S_0, I_0, S_1, I_1) .

Peak estimation is employed to bound the maximum infection rate over the course of the epidemic. This peak estimation program maximizes $\langle I, \mu_p \rangle$ under the constraint that $(\mu_p, \bar{\mu}, \{\nu_0, \nu_1\}, \hat{\nu}_1)$ is a free-time MV-solution of dynamics (25).

Figure 6 displays the output of peak estimation, where the order-3 LMI relaxation bounds the maximal infection rate at 56.89%. The moment matrix $\mathbb{M}_3[y_p]$ is approximately rank-1 (second largest eigenvalue of $\mathbb{M}_3[y_p] = 2.448 \times 10^{-5}$), and the extracted optimum from $\mathbb{M}_3[y_p]$ by Algorithm 1 of [18] is $(S^*, I^*) = (0.0561, 0.5689)$ occurring at $t^* = 15.636$ days.

5.2 Delayed Flow System

A time-delayed version of the Flow system from [15] is

$$\dot{x}(t) = \begin{bmatrix} x_2(t) \\ -x_1(t - \tau) - x_2(t) + x_1(t)^3/3 \end{bmatrix}. \quad (26)$$

Figure 7 plots the delayed Flow system (26) without lag ($\tau = 0$ in blue) and with a lag ($\tau = 0.75$ in orange) starting from the constant initial history $x_h(t) = (1.5, 0), \forall t \in [-\tau, 0]$ (black circle).

The time-zero set of allowable histories is $X_0 = \{x \in \mathbb{R}^2 \mid (x_1 - 1.5)^2 + x_2^2 \leq 0.4^2\}$. The history class \mathcal{H} will be the set of functions $x_h \in PC([-\tau, 0])$ whose graphs $(t, x(t))$ are contained within the cylinder $H_0 = [-0.75, 0] \times X_0$. No further requirements of continuity are posed on histories in \mathcal{H} . The considered peak estimation aims to find the minimum value of x_2 (maximize $p(x) = -x_2$) for trajectories following (26) starting from H_0 , within the state set $X = [-1.25, 2.5] \times [-1.25, 1.5]$ and time horizon $T = 5$. The first five bounds on the maximum value of $-x_2$ by solving (21) are $p_{1:5}^* = [1.25, 1.2183, 1.1913, 1.1727, 1.1630]$.

Figure 8 plots trajectories and peak information associated with this example. The black circle is the initial set X_0 . The initial histories inside X_0 are plotted in grey. These sampled histories are piecewise constant with 10 uniformly spaced jumps (moving to a new point uniformly sampled in X_0) within $[-0.75, 0]$.

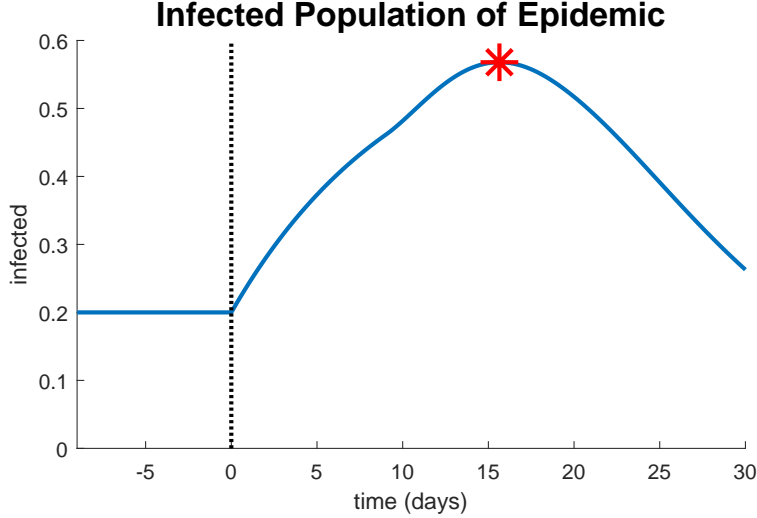


Figure 6: SIR peak estimation and recovery at order 3

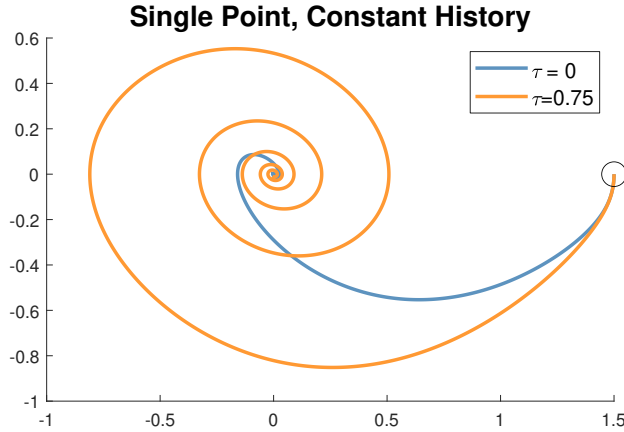


Figure 7: Comparison of delayed Flow systems (26) with lags $\tau = 0$ and $\tau = 0.75$ in times $t \in [0, 20]$

The cyan curves are the DDE trajectories of (26) starting from the grey histories. The red dotted line is the p_5^* bound on the minimum vertical coordinate of a point on any trajectory starting from \mathcal{H} up to $T = 5$.

Distance estimation is performed on the Flow system 26 with an L_2 metric, a time horizon of $T = 8$, arbitrarily varying histories in H_0 , a time horizon of $\tau = 0.5$, and a half-circle unsafe set $X_u = \{x \mid 0.5^2 \geq (x_1 + 0.5)^2 + (x_2 + 1)^2, (1.5 + x_1 + x_2)\}$. The recovered distance estimates up to degree 4 from SDP relaxations of (24) are $c_{1:4}^* = [1.1897 \times 10^{-4}, 4.0420 \times 10^{-4}, 0.1572, 0.1820]$. Figure 9 plots the set X_u in red along with its $c_4^* = 0.1820$ certified distance contour.

5.3 Delayed Time-Varying System

This example involves peak estimation of a DDE version of the time-varying Example 2.1 of [6] with

$$\dot{x}(t) = \begin{bmatrix} x_2(t)t - 0.1x_1(t) - x_1(t-\tau)x_2(t-\tau) \\ -x_1(t)t - x_2(t) + x_1(t)x_1(t-\tau) \end{bmatrix}. \quad (27)$$

The considered support parameters are $\tau = 0.75$, $T = 5$, and $X = [-1.25, 1.25] \times [-0.75, 1.25]$. The time-zero set is the disk $X_0 = \{x \in \mathbb{R}^2 \mid (x_1 + 0.75)^2 + x_2^2 \leq 0.3^2\}$. The only restriction on allowable histories \mathcal{H} is that their graphs are contained in the history set $H_0 = [-0.75, 0] \times X_0$.

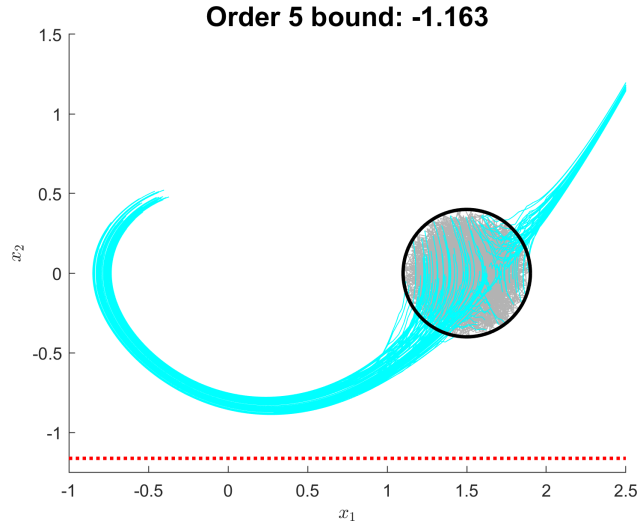


Figure 8: Minimize x_2 on the delayed Flow system (26)

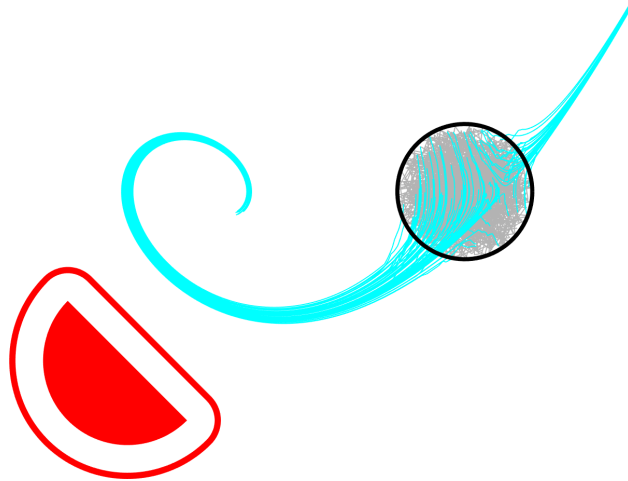


Figure 9: Minimize $c(x; X_u)$ on the delayed Flow system (26)

Solving the SDP associated with the LMI (21) to maximize the peak function $p = x_1$ yields the sequence of five bounds $p_{1:5}^* = [1.25, 1.25, 1.1978, 0.8543, 0.718264618]$. Figure 10 plots system trajectories and the p_5^* bound on x_1 using the same visual convention as Figure 8 (black circle X_0 , grey histories $x_h(t)$, cyan trajectories $x(t | x_h)$, red dotted line $x_1 = p_5^*$).

Figure 11 plots the corresponding trajectory and bound information in 3d (t, x_1, x_2) . The black circles denote the boundary of H_0 . The history structure inside H_0 between times $[-0.75, 1]$ is clearly visible in grey.

The peak estimation of $p = x_2$ under the same system parameters leads to the sequence of five bounds $p_{1:5}^* = [1.25, 1.25, 0.9557, 0.9138, 0.9112]$.

6 Extensions

This section discusses several extensions to the DDE peak estimation framework.

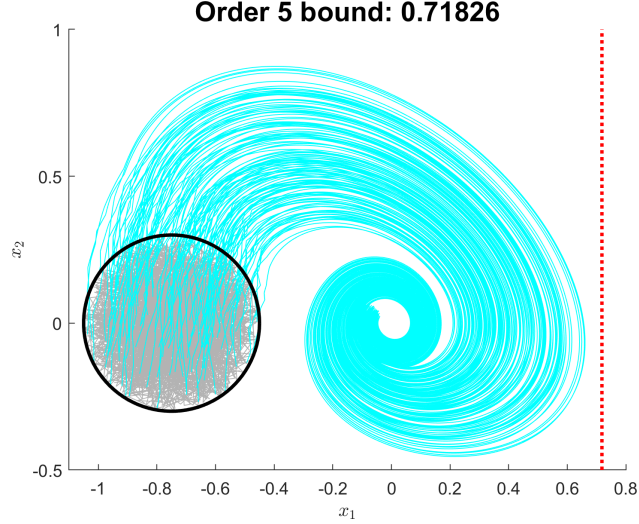


Figure 10: Maximize x_1 on the delayed time-varying (27)

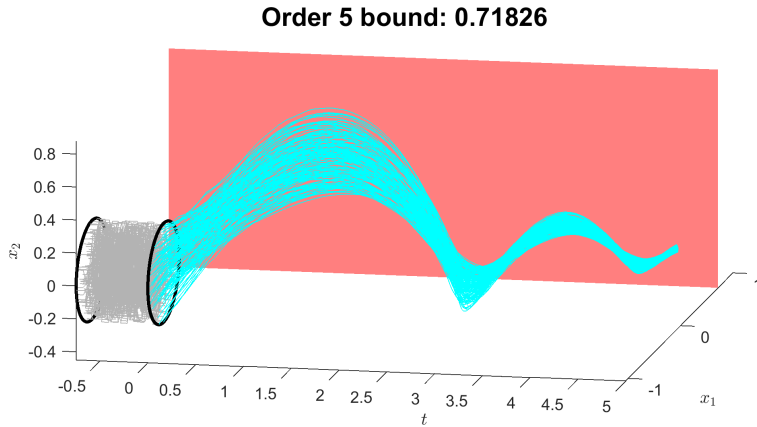


Figure 11: A 3d plot of (27) and its x_1 bound

6.1 Shaping Constraints

Assumption A5 imposes that the class \mathcal{H} is graph-constrained. Some applications involve further structure in the function class \mathcal{H} , such as requiring that the histories in \mathcal{H} are constant in time between $t \in [-\tau_r, 0]$. Examples of these constant histories for the system in (2) starting within the black box (H_0) are plotted in Figure 12.

These types of structure in histories may be realized by adding constraints to μ_h . A method to ensure that the histories in μ_h are constant in time between $t \in [-\tau, 0]$ is by requiring μ_h to be the occupation measure of the system $\dot{x} = 0$ through a Liouville equation

$$\langle v(0, x), \mu_0 \rangle = \langle \partial_t v(t, x), \mu_h \rangle + \langle v(-\tau, x), \mu_0 \rangle \quad \forall v \in C([-\tau_r, 0]). \quad (28)$$

6.2 Multiple Time Delays

A DDE with multiple time-delays $0 < \tau_1 < \tau_2 < \dots < \tau_r$ for (r, τ_r) finite and a history $x_h \in PC([-\tau_r, 0], X)$ is

$$\begin{aligned} \dot{x}(t) &= f(t, x(t), x(t - \tau_1), \dots, x(t - \tau_r)) \\ x(t) &= x_h(t), \quad \forall t \in [-\tau_r, 0]. \end{aligned} \quad (29)$$

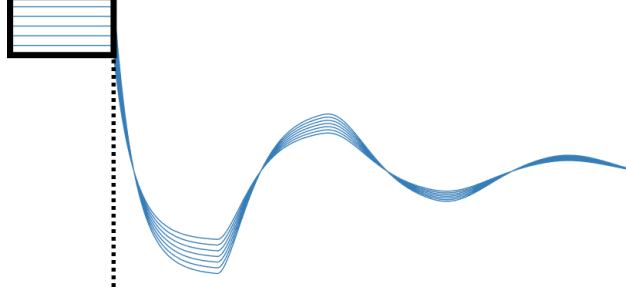


Figure 12: Constant histories in the black box

A peak estimation problem for (29) with history class \mathcal{H} and objective $p(x)$ is

$$P^* = \sup_{t^* \in [0, T], x_h(\cdot)} p(x(t^* | x_h)) \quad (30a)$$

$$\dot{x} = f(t, x(t), x(t - \tau_1), \dots, x(t - \tau_r)) \quad \forall t \in [0, T] \quad (30b)$$

$$x(t) = x_h(t) \quad \forall t \in [-\tau_r, 0] \quad (30c)$$

$$x_h(\cdot) \in \mathcal{H}. \quad (30d)$$

A multiple-time-delay MV-solution for the peak estimation problem (30) is (for all $i = 1..r$):

$$\text{History} \quad \mu_{hi} \in \mathcal{M}_+(H_0 \cap ([-\tau_i, -\tau_{i-1}] \times X)) \quad (31a)$$

$$\text{Initial} \quad \mu_0 \in \mathcal{M}_+(X_0) \quad (31b)$$

$$\text{Peak} \quad \mu_p \in \mathcal{M}_+([0, T] \times X) \quad (31c)$$

$$\text{Time-Slack} \quad \nu_i \in \mathcal{M}_+([0, T] \times X) \quad (31d)$$

$$\text{Occupation Start} \quad \bar{\mu}_0 \in \mathcal{M}_+([0, T - \tau] \times X^2) \quad (31e)$$

$$\text{Occupation End} \quad \bar{\mu}_i \in \mathcal{M}_+([T - \tau_i, T - \tau_{i-1}] \times X^2). \quad (31f)$$

The Lie derivative operator \mathcal{L}_f with respect to (29) for $v \in C^1([0, T] \times X)$ is

$$\mathcal{L}_f v(t, x_0) = \partial_t v(t, x_0) + f(t, x_0, x_1, \dots, x_r) \cdot \nabla_{x_0} v(t, x_0). \quad (32)$$

The multiple-time-delay peak estimation LP for (30) problem of $p(x)$ is

$$p^* = \sup \langle p, \mu_p \rangle \quad (33a)$$

$$\langle 1, \mu_0 \rangle = 1 \quad (33b)$$

$$\pi_{\#}^t \mu_{hi} = \lambda_{[-\tau_i, -\tau_{i-1}]} \quad \forall i = 1..r \quad (33c)$$

$$\mu_p = \delta_0 \otimes \mu_0 + \pi_{\#}^{tx_0} \mathcal{L}_f^{\dagger} (\bar{\mu}_0 + \sum_{i=1}^r \bar{\mu}_i) \quad (33d)$$

$$\pi_{\#}^{tx_1} (\bar{\mu}_0 + \sum_{i=1}^r \bar{\mu}_i) + \nu_i = S_{\#}^{\tau_i} (\sum_{j=1}^i \mu_{hj} + \pi_{\#}^{tx_0} (\bar{\mu}_0 + \sum_{j=1}^{i-1} \bar{\mu}_i)) \quad \forall i = 1..r \quad (33e)$$

$$\text{Measure Definitions from (31)}. \quad (33f)$$

Theorem 3.2 can be extended to the multiple-time-delay case to prove that $P^* \leq p^*$ between (30) and (33). Even if Conjecture 3.1 holds in the single-delay case, it is unlikely the conjecture is satisfied in the multiple-delay case due to findings in [12].

6.3 Uncertainty

This extension subsection will discuss three types of uncertainty that can affect DDEs dynamics: time-independent, time-dependent, and unknown-delay.

6.3.1 Time-independent Uncertainty

Time-independent uncertainty $\theta \in \Theta$ for a set Θ can be added to dynamics by adjoining the state θ following $\dot{\theta} = 0$ to (1b). This same process occurs in [36] for the ODE case.

6.3.2 Time-dependent Uncertainty

Time-dependent may be implemented by a Young Measure approach. Given dynamics $\dot{x}(t) = f(t, x(t), x(t-\tau), w(t))$ for $w(t) \in W$, the joint occupation measures representing trajectories are $\bar{\mu}_0 \in \mathcal{M}_+([0, T-\tau] \times X^2 \times W)$ and $\bar{\mu}_1 \in \mathcal{M}_+([T-\tau, T] \times X^2 \times W)$. No substantial changes are required to the Liouville nor consistency constraints.

Input delays may also be introduced into dynamics with $\dot{x}(t) = f(t, x(t), x(t-\tau), w(t), w(t-\tau))$ under the state history x_h and input history w_h (defined in times $t \in [-\tau, 0]$). The associated joint occupation measures are now $\bar{\mu}_0 \in \mathcal{M}_+([0, T-\tau] \times X^2 \times W^2)$ and $\bar{\mu}_1 \in \mathcal{M}_+([T-\tau, T] \times X^2 \times W^2)$, each involving variables (t, x_0, x_1, w_0, w_1) . The state-input history class is $\mathcal{H} \in PC([-\tau, 0], X \times W)$, and its history occupation measure now includes an input component $\mu_h \in \mathcal{M}_+([-\tau, 0] \times X \times W)$.

While the Liouville equation stays the same as (11), the consistency constraint ensures that the w_1 coordinate contains a delayed copy of w_0 ,

$$\pi_{\#}^{tx_1w_1}(\bar{\mu}_0 + \bar{\mu}_1) = S_{\#}^{\tau}(\mu_h + \pi^{tx_0w_0}\bar{\mu}_0). \quad (34)$$

6.3.3 Unknown Delays

This extension focuses on dynamics where the time-independent (constant) delay is unknown but fixed in the finite range of $\tau \in [\underline{\tau}, \bar{\tau}]$. The unknown delay τ must be treated as an additional state with $\dot{\tau} = 0$.

The following sets may be defined:

$$\Omega_h = \{(\tau, t, x) \mid \tau \in [\underline{\tau}, \bar{\tau}], (t, x) \in H_0 \mid_{\tau}\} \quad (35a)$$

$$\Omega_0 = \{(\tau, t, x_0, x_1) \mid \tau \in [\underline{\tau}, \bar{\tau}], t \in [0, T-\tau], (x_0, x_1) \in X^2\} \quad (35b)$$

$$\Omega_1 = \{(\tau, t, x_0, x_1) \mid \tau \in [\underline{\tau}, \bar{\tau}], t \in [T-\tau, T], (x_0, x_1) \in X^2\}. \quad (35c)$$

A MV-solution in the unknown-delay case has the form:

$$\text{History} \quad \mu_h \in \mathcal{M}_+(\Omega_h) \quad (36a)$$

$$\text{History Slack} \quad \bar{\mu}_h \in \mathcal{M}_+(\Omega_h) \quad (36b)$$

$$\text{Initial} \quad \mu_0 \in \mathcal{M}_+(X_0 \times [\underline{\tau}, \bar{\tau}]) \quad (36c)$$

$$\text{Peak} \quad \mu_p \in \mathcal{M}_+([0, T] \times X \times [\underline{\tau}, \bar{\tau}]) \quad (36d)$$

$$\text{Time-Slack} \quad \nu \in \mathcal{M}_+([0, T] \times X \times [\underline{\tau}, \bar{\tau}]) \quad (36e)$$

$$\text{Occupation Start} \quad \bar{\mu}_0 \in \mathcal{M}_+(\Omega_0) \quad (36f)$$

$$\text{Occupation End} \quad \bar{\mu}_1 \in \mathcal{M}_+(\Omega_1). \quad (36g)$$

The Liouville and Consistency constraints in the unknown-delay case are unchanged as compared to the known-delay system (with the new state $\dot{\tau} = 0$).

However, the history-validity constraints have the following form,

$$\langle 1, \mu_0 \rangle = 1 \quad (37a)$$

$$\delta_{t=0} \otimes (\pi_{\#}^{\tau} \mu_0) = \delta_{t=-\bar{\tau}} \otimes (\pi_{\#}^{\tau} \mu_0) + (\partial_t)_{\#} (\pi_{\#}^{t\tau} (\mu_h + \hat{\mu}_h)) \quad (37b)$$

$$\pi^t (\mu_h + \hat{\mu}_h) = \lambda_{[-\bar{\tau}, 0]}. \quad (37c)$$

Constraint (37a) ensures that the initial distribution μ_0 is a probability measure. Constraint (37b) imposes that $\tau(t)$ is constant in time between $t = [-\bar{\tau}, 0]$. Constraint (37c) is a domination term that requires the history x_h to be defined in times $[-\bar{\tau}, 0]$.

It is an open problem to extend consistency constraints and MV-solutions towards cases where the delay $\tau(t)$ is time-dependent (such as $\tau(t) \in [-B, B]$).

7 Conclusion

This paper presented a formulation of MV-solutions for free-terminal-time DDEs with multiple histories (Definition 3.1). These MV-solutions are formed by the conjunction of Validity, Liouville and Consistency constraints. These MV-solutions may be used to provide upper bounds on peak estimation problems over DDEs by Program (17).

A vital area for future work is determining the conditions under which $P^* = p^*$ between (1) and (17) (Conjecture 3.1). Other areas for future work include applying MV-solutions to other problems (such as reachable set and positive-invariant set estimation) and formulating delay-dependent MV-solutions.

Acknowledgements

The authors thank Corbinian Schlosser, Matteo Tacchi, Didier Henrion, Leonid Mirkin, Alexandre Seuret, and Sabine Mondié for their discussions about DDEs and occupation measures.

References

- [1] J. K. Hale, “Functional Differential Equations,” in *Analytic Theory of Differential Equations*. Springer, 1971, pp. 9–22.
- [2] Y. Kuang, *Delay Differential Equations: with Applications in Population Dynamics*. Academic Press, 1993.
- [3] A. Bellen and M. Zennaro, *Numerical Methods for Delay Differential Equations*. Oxford University Press, 2013.
- [4] E. Fridman, *Introduction to Time-Delay Systems: Analysis and Control*. Birkhäuser Basel, 10 2014.
- [5] M. J. Cho and R. H. Stockbridge, “Linear Programming Formulation for Optimal Stopping Problems,” *SIAM Journal on Control and Optimization*, vol. 40, no. 6, pp. 1965–1982, 2002.
- [6] G. Fantuzzi and D. Goluskin, “Bounding Extreme Events in Nonlinear Dynamics Using Convex Optimization,” *SIAM Journal on Applied Dynamical Systems*, vol. 19, no. 3, pp. 1823–1864, 2020.
- [7] J. Warga, “Optimal Controls with Pseudodelays,” *SIAM Journal on Control*, vol. 12, no. 2, pp. 286–299, 1974.
- [8] L. C. Young, “Generalized Surfaces in the Calculus of Variations,” *Annals of Mathematics*, vol. 43, pp. 84–103, 1942.
- [9] J. Warga, *Optimal control of differential and functional equations*. Academic press, 2014.
- [10] J. F. Rosenblueth and R. B. Vinter, “Relaxation Procedures for Time Delay Systems,” *Journal of Mathematical Analysis and Applications*, vol. 162, no. 2, pp. 542–563, 1991.
- [11] J. F. Rosenblueth, “Strongly and weakly relaxed controls for time delay systems,” *SIAM Journal on Control and Optimization*, vol. 30, no. 4, pp. 856–866, 1992.
- [12] J. Rosenblueth, “Proper relaxation of optimal control problems,” *Journal of Optimization Theory and Applications*, vol. 74, no. 3, pp. 509–526, 1992.
- [13] R. Lewis and R. Vinter, “Relaxation of Optimal Control Problems to Equivalent Convex Programs,” *Journal of Mathematical Analysis and Applications*, vol. 74, no. 2, pp. 475–493, 1980.
- [14] J. B. Lasserre, *Moments, Positive Polynomials And Their Applications*, ser. Imperial College Press Optimization Series. World Scientific Publishing Company, 2009.

- [15] S. Prajna and A. Jadbabaie, “Safety Verification of Hybrid Systems Using Barrier Certificates,” in *International Workshop on Hybrid Systems: Computation and Control*. Springer, 2004, pp. 477–492.
- [16] D. Henrion, J. B. Lasserre, and C. Savorgnan, “Nonlinear optimal control synthesis via occupation measures,” in *2008 47th IEEE Conference on Decision and Control*. IEEE, 2008, pp. 4749–4754.
- [17] A. Papachristodoulou, M. M. Peet, and S. Lall, “Analysis of Polynomial Systems With Time Delays via the Sum of Squares Decomposition,” *IEEE Transactions on Automatic Control*, vol. 54, no. 5, pp. 1058–1064, 2009.
- [18] J. Miller, D. Henrion, and M. Sznaier, “Peak Estimation Recovery and Safety Analysis,” *IEEE Control Systems Letters*, vol. 5, no. 6, pp. 1982–1987, 2020.
- [19] M. Korda, D. Henrion, and C. N. Jones, “Inner approximations of the region of attraction for polynomial dynamical systems,” *IFAC Proceedings Volumes*, vol. 46, no. 23, pp. 534–539, 2013.
- [20] V. Magron, P.-L. Garoche, D. Henrion, and X. Thirioux, “Semidefinite Approximations of Reachable Sets for Discrete-time Polynomial Systems,” *SIAM J. Control Optim.*, vol. 57, pp. 2799–2820, 03 2017.
- [21] J. Miller and M. Sznaier, “Bounding the Distance of Closest Approach to Unsafe Sets with Occupation Measures,” in *2022 61st IEEE Conference on Decision and Control (CDC)*, 2022, pp. 5008–5013.
- [22] A. Papachristodoulou and S. Prajna, “A Tutorial on Sum of Squares Techniques for Systems Analysis,” in *Proceedings of the 2005, American Control Conference, 2005*. IEEE, 2005, pp. 2686–2700.
- [23] S. Prajna and A. Jadbabaie, “Methods for Safety Verification of Time-Delay Systems,” in *Proceedings of the 44th IEEE Conference on Decision and Control*. IEEE, 2005, pp. 4348–4353.
- [24] S. Marx, T. Weisser, D. Henrion, and J. B. Lasserre, “A moment approach for entropy solutions to nonlinear hyperbolic PDEs,” *Mathematical Control and Related Fields*, vol. 10, no. 1, pp. 113–140, 2020.
- [25] M. Korda, D. Henrion, and J. B. Lasserre, “Chapter 10 - Moments and convex optimization for analysis and control of nonlinear pdes,” in *Numerical Control: Part A*, ser. Handbook of Numerical Analysis, E. Trélat and E. Zuazua, Eds. Elsevier, 2022, vol. 23, pp. 339–366.
- [26] V. Magron and C. Prieur, “Optimal Control of Linear PDEs using Occupation Measures and SDP Relaxations,” *IMA Journal of Mathematical Control and Information*, vol. 37, no. 1, pp. 159–174, 2020.
- [27] S. Barati, “Optimal Control of Constrained Time Delay Systems,” *Advanced Modeling and Optimization*, vol. 14, no. 1, pp. 103–116, 2012.
- [28] R. Suresh and V. K. Chandrasekar, “Influence of time-delay feedback on extreme events in a forced Liénard system,” *Phys. Rev. E*, vol. 98, p. 052211, Nov 2018.
- [29] M. Sadeghi, J. M. Greene, and E. D. Sontag, “Universal features of epidemic models under social distancing guidelines,” *Annual Reviews in Control*, 2021.
- [30] T. Tao, *An Introduction to Measure Theory*. American Mathematical Society Providence, RI, 2011, vol. 126.
- [31] M. Tacchi, “Convergence of Lasserre’s hierarchy: the general case,” *Optimization Letters*, vol. 16, no. 3, pp. 1015–1033, 2022.
- [32] D. Henrion and J.-B. Lasserre, “GloptiPoly: Global Optimization over Polynomials with Matlab and SeDuMi,” *ACM Transactions on Mathematical Software (TOMS)*, vol. 29, no. 2, pp. 165–194, 2003.
- [33] J. Löfberg, “YALMIP : A Toolbox for Modeling and Optimization in MATLAB,” in *In Proceedings of the CACSD Conference*, Taipei, Taiwan, 2004.

- [34] M. ApS, *The MOSEK optimization toolbox for MATLAB manual. Version 9.2.*, 2020. [Online]. Available: <https://docs.mosek.com/9.2/toolbox/index.html>
- [35] S. A. Lauer, K. H. Grantz, Q. Bi, F. K. Jones, Q. Zheng, H. R. Meredith, A. S. Azman, N. G. Reich, and J. Lessler, “The incubation period of coronavirus disease 2019 (covid-19) from publicly reported confirmed cases: estimation and application,” *Annals of internal medicine*, vol. 172, no. 9, pp. 577–582, 2020.
- [36] J. Miller, D. Henrion, M. Sznaier, and M. Korda, “Peak Estimation for Uncertain and Switched Systems,” in *2021 60th IEEE Conference on Decision and Control (CDC)*, 2021, pp. 3222–3228.
- [37] J. R. Ockendon and A. B. Tayler, “The dynamics of a current collection system for an electric locomotive,” *Proceedings of the Royal Society of London. A. Mathematical and Physical Sciences*, vol. 322, no. 1551, pp. 447–468, 1971.
- [38] J. Carr and J. Dyson, “2.-the matrix functional differential equation $y'(x) = \lambda y(x) + b y(x)$,” *Proceedings of the Royal Society of Edinburgh Section A: Mathematics*, vol. 75, no. 1, pp. 5–22, 1976.
- [39] A. Iserles, *On the generalized pantograph functional-differential equation*. University of Cambridge, Department of Applied Mathematics and Theoretical, 1991.
- [40] —, “On nonlinear delay differential equations,” *Transactions of the American Mathematical Society*, vol. 344, no. 1, pp. 441–477, 1994.
- [41] Y. Liu, “Asymptotic behaviour of functional-differential equations with proportional time delays,” *European Journal of Applied Mathematics*, vol. 7, no. 1, pp. 11–30, 1996.
- [42] L. Shampine, “Solving odes and ddes with residual control,” *Applied Numerical Mathematics*, vol. 52, no. 1, pp. 113–127, 2005.
- [43] I. Ali, H. Brunner, and T. Tang, “A spectral method for pantograph-type delay differential equations and its convergence analysis,” *Journal of Computational Mathematics*, pp. 254–265, 2009.
- [44] S. Sedaghat, Y. Ordokhani, and M. Dehghan, “Numerical solution of the delay differential equations of pantograph type via chebyshev polynomials,” *Communications in Nonlinear Science and Numerical Simulation*, vol. 17, no. 12, pp. 4815–4830, 2012.
- [45] M. M. Bahşı and M. Çevik, “Numerical solution of pantograph-type delay differential equations using perturbation-iteration algorithms,” *Journal of Applied Mathematics*, 2015.
- [46] M. Tacchi, “Moment-sos hierarchy for large scale set approximation. application to power systems transient stability analysis,” Ph.D. dissertation, Toulouse, INSA, 2021.
- [47] A. Plaksin, “Minimax and Viscosity Solutions of Hamilton–Jacobi–Bellman Equations for Time-Delay Systems,” *Journal of Optimization Theory and Applications*, vol. 187, no. 1, pp. 22–42, 2020.
- [48] O. Santos, S. Mondié, and V. L. Kharitonov, “Linear quadratic suboptimal control for time delays systems,” *International Journal of Control*, vol. 82, no. 1, pp. 147–154, 2009.
- [49] J.-M. Ortega-Martínez, O.-J. Santos-Sánchez, and S. Mondié, “Comments on the bellman functional for linear time-delay systems,” *Optimal Control Applications and Methods*, vol. 42, no. 5, pp. 1531–1540, 2021.
- [50] D. Liberzon, *Calculus of Variations and Optimal Control Theory: A Concise Introduction*. Princeton University Press, 2011.
- [51] M. Jones and M. M. Peet, “Polynomial Approximation of Value Functions and Nonlinear Controller Design with Performance Bounds,” 2021.

A Delay Structures

This chapter has focused on supremizing $p(x)$ in (1) over continuous-time systems with a discrete delay $x(t - \tau)$. This subsection will discuss peak estimation of $p(x)$ with respect to other types of dynamics and delay structures.

A.1 Proportional Time-Delays

A system with a proportional delay is defined with respect to a scaling term $\kappa \in [0, 1]$:

$$\dot{x}(t) = f(t, x(t), x(\kappa t)). \quad (38)$$

Proportional time delays are observed in the current collection of a pantograph on a streetcar [37]. References on functional differential equation with proportional time delay include [38, 39, 40, 41]. MATLAB uses the command `ddesd` to solve DDEs with time-dependent delays by an RK4 algorithm [42]. Other numerical algorithms specifically for proportional delays include [43, 44, 45].

The peak estimation problem over (38) is,

$$P^* = \sup_{t^* \in [0, T], x_0 \in X_0} p(x(t^* | x_0)) \quad (39a)$$

$$\dot{x} = f(t, x(t), x(\kappa t)) \quad \forall t \in [0, T]. \quad (39b)$$

A MV-solution for proportional time delays is

$$\text{Initial} \quad \mu_0 \in \mathcal{M}_+(X_0) \quad (40a)$$

$$\text{Peak} \quad \mu_p \in \mathcal{M}_+([0, T] \times X) \quad (40b)$$

$$\text{Time-Slack} \quad \nu \in \mathcal{M}_+([0, T] \times X) \quad (40c)$$

$$\text{Occupation Start} \quad \bar{\mu}_0 \in \mathcal{M}_+([0, \kappa T] \times X^2) \quad (40d)$$

$$\text{Occupation End} \quad \bar{\mu}_1 \in \mathcal{M}_+([\kappa T, T] \times X^2). \quad (40e)$$

Note how the MV-solution (40) lacks a history measure μ_h as compared with (9), and also how the limits on (40d)-(40e) are $[0, \kappa T]$ and $[\kappa T, T]$ respectively.

The Lie derivative operator \mathcal{L} with $\mathcal{L}v = (\partial_t + f(t, x_0, x_1) \cdot \nabla_{x_0})v(t, x_0)$ is the same as in the discrete-delay case (11), but under dynamics (38).

The consistency constraint follows from a modification of Lemma 3.1:

Lemma A.1. *Let $x(\cdot)$ be a solution to (39b) with an initial condition of $x_0 \in X_0$ and a stopping time of $t^* \in [0, T]$. The following pairs of integral are equal for all $\phi \in C([0, T] \times X)$:*

$$\int_0^{t^*} \phi(t, x(\kappa t)) dt = \frac{1}{\kappa} \int_0^{\min(t^*/\kappa, T)} \phi(t'/\kappa, x(t)) dt'. \quad (41)$$

Proof. This relation is due to a change of variable with $t' \leftarrow \kappa t$. \square

The resultant consistency constraint w.r.t. the measures in (40) is

$$\langle \phi(t, x_1), \bar{\mu}_0 + \bar{\mu}_1 \rangle + \langle \phi(t, x), \nu \rangle = \langle \phi(t/\kappa, x_0)/\kappa, \bar{\mu}_0 \rangle. \quad (42)$$

Expressing the linear expansion operator E_κ as $E_\kappa \phi(t, x) = \phi(t/\kappa, x_0)\kappa$, the measure LP for problem (39) is,

$$p^* = \sup \langle p, \mu_p \rangle \quad (43a)$$

$$\langle 1, \mu_0 \rangle = 1 \quad (43b)$$

$$\mu_p = \delta_0 \otimes \mu_0 + \pi_{\#}^{tx_0} \mathcal{L}_f^\dagger (\bar{\mu}_0 + \bar{\mu}_1) \quad (43c)$$

$$\pi_{\#}^{tx_1} (\bar{\mu}_0 + \bar{\mu}_1) + \nu = E_{\#}^\kappa (\pi_{\#}^{tx_0} \bar{\mu}_0) \quad (43d)$$

$$\text{Measure Definitions from (40)}. \quad (43e)$$

Problem (43) upper-bounds (39) by following the reasoning from Theorem 3.2 for the proportional-delay case.

Remark 6. *Proportional and discrete delays can be applied together to form dynamics,*

$$\dot{x}(t) = f(t, x(t), x(\kappa t - \tau)). \quad (44)$$

Causality of (44) requires that $\kappa \in [0, 1)$ and $\tau \geq 0$. A consistency constraint may be posed using an integral relation

$$\int_0^T \phi(t, x(\kappa t - \tau)) dt = \int_{-\tau}^{\kappa T - \tau} \phi((t + \tau)/\kappa, x(t))/\kappa dt, \quad (45)$$

used as a step towards forming Lemmas 3.1 and A.1.

A.2 Discrete-Time Systems

This subsection will concentrate on a discrete-time system with a long time delay. The discrete-time system $x[t]$ is defined w.r.t. a delay $\tau \in \mathbb{N}$, and a time horizon $T \in \mathbb{N}$ under the assumption that $\tau < T$.

The peak estimation program for a system with discrete-time dynamics and one time delay τ is:

$$P^* = \sup_{t^* \in 0..T, x_h[\cdot]} p(x[t | x_h]) \quad (46a)$$

$$\dot{x} = f(t, x[t], x[t - \tau]) \quad \forall t \in 1..T \quad (46b)$$

$$x[t] = x_h[t] \quad \forall t \in [-\tau, 0] \quad (46c)$$

$$x_h[\cdot] \in \mathcal{H}. \quad (46d)$$

Delayed dynamics (46b) may be implemented as a non-delayed discrete system by state inflation in terms of $x[t - (0..\tau)]$ [4]. Such state augmentation could lead to a large number of variables in systems analysis and result in intractably large computational problems.

This subsection will define a MV-solution using the variables from (9), in which the measures with the maximum number of variables are $(\bar{\mu}_0(t, x_0, x_1), \bar{\mu}_1(t, x_0, x_1))$.

A.2.1 History-Validity

The history-validity constraint for discrete-time systems will separate the history $x_h[t]$ into a time-zero component (μ_0) and a history component $t \in -\tau..-1$ (μ_h). The time-zero component is $\mu_0 \in X_0$, as in Section 3.2.1.

The history measure μ_h should represent a history $x_h[t]$ defined between $t \in -\tau..-1$. This may be imposed by setting the t -marginal of μ_h to a train of Dirac-deltas supported at sample times $-\tau..-1$,

$$\pi_{\#}^t \mu_h = \sum_{t=-\tau}^{-1} \delta_t. \quad (47)$$

A.2.2 Liouville

The discrete-time Liouville equation [20] applied to the dynamics (46b) for all test functions $v \in C([0, T + 1] \times X)$ is,

$$\langle v(t, x), \mu_p \rangle = \langle v(0, x), \mu_0 \rangle + \langle v(t + 1, f(t, x_0, x_1) - v(t, x_0, x_1), \bar{\mu}_0 + \bar{\mu}_1 \rangle. \quad (48)$$

The Liouville constraint in (48) will be abbreviated (using the identity operator $Id(x) = x$),

$$\mu_p = \delta_0 \otimes \mu_0 + \pi_{\#}^{tx_0} ((t + 1, f)_{\#} - Id_{\#})(\bar{\mu}_0 + \bar{\mu}_1). \quad (49)$$

A.2.3 Consistency

The consistency constraint for dynamics (46b) may be derived from the following Lemma,

Lemma A.2. Let $x[\cdot]$ be a trajectory of (46b) given an initial history x_h and a stopping time of $t^* \in 0..T$. It follows that the below pair of summations are equal for all $\phi \in C([0, T] \times X)$:

$$\left(\sum_{t=0}^{t^*} + \sum_{t=t^*}^{\min(T, t^* + \tau)} \right) \phi(t, x[t - \tau]) dt = \sum_{t'=-\tau}^{\min(T-\tau, t^*)} \phi(t' + \tau, x[t']). \quad (50)$$

Proof. The index of summation is exchanged as $t' \rightarrow t - \tau$. \square

The resultant consistency constraint from Lemma A.2 has an identical form as (16) with

$$\pi_{\#}^{tx_1}(\bar{\mu}_0 + \bar{\mu}_1) + \nu = S_{\#}^{\tau}(\mu_h + \pi^{tx_0} \bar{\mu}_0). \quad (51)$$

A.2.4 Measure Program

The peak estimation measure LP that upper-bounds (46) is,

$$p^* = \sup \langle p, \mu_p \rangle \quad (52a)$$

$$\langle 1, \mu_0 \rangle = 1 \quad (52b)$$

$$\pi_{\#}^t \mu_h = \sum_{t'=-\tau}^{-1} \delta_{t=t'} \quad (52c)$$

$$\mu_p = \delta_0 \otimes \mu_0 + \pi_{\#}^{tx_0}((t+1, f, x_1)_{\#} - Id_{\#})(\bar{\mu}_0 + \bar{\mu}_1) \quad (52d)$$

$$\pi_{\#}^{tx_1}(\bar{\mu}_0 + \bar{\mu}_1) + \nu = S_{\#}^{\tau}(\mu_h + \pi_{\#}^{tx_0} \bar{\mu}_0) \quad (52e)$$

$$\text{Measure Definitions from (9)}. \quad (52f)$$

This upper-bound also follows from constructing measures from trajectories as in Theorem 3.2.

B Proof of Strong Duality

This appendix will prove strong duality between programs (17) and (18) for peak estimation. The general pattern for cone conventions and affine maps of [46] will be followed.

The signed measure spaces of (9) are

$$\begin{aligned} \mathcal{X} &= \mathcal{M}(H_0) \times \mathcal{M}(X_0) \times \mathcal{M}([0, T] \times X)^2 \\ &\quad \times \mathcal{M}([0, T - \tau] \times X^2) \times \mathcal{M}([T - \tau, T] \times X^2) \\ \mathcal{X}' &= \mathcal{C}(H_0) \times \mathcal{C}(X_0) \times \mathcal{C}([0, T] \times X)^2 \\ &\quad \times \mathcal{C}([0, T - \tau] \times X^2) \times \mathcal{C}([T - \tau, T] \times X^2). \end{aligned} \quad (53)$$

Their nonnegative subcones (with (9) membership) are topological duals under A1 and have definitions

$$\begin{aligned} \mathcal{X}_+ &= \mathcal{M}_+(H_0) \times \mathcal{M}_+(X_0) \times \mathcal{M}_+([0, T] \times X)^2 \\ &\quad \times \mathcal{M}_+([0, T - \tau] \times X^2) \times \mathcal{M}_+([T - \tau, T] \times X^2) \\ \mathcal{X}'_+ &= \mathcal{C}_+(H_0) \times \mathcal{C}_+(X_0) \times \mathcal{C}_+([0, T] \times X)^2 \\ &\quad \times \mathcal{C}_+([0, T - \tau] \times X^2) \times \mathcal{C}_+([T - \tau, T] \times X^2). \end{aligned} \quad (54)$$

The collection of measures in (9) will be denoted as $\boldsymbol{\mu} = (\mu_h, \mu_0, \mu_p, \nu, \bar{\mu}_0, \bar{\mu}_1)$ and is a member of \mathcal{X}_+ .

The constraint spaces of (17b)-(17e) are

$$\mathcal{Y} = \mathbb{R} \times \mathcal{C}([-\tau, 0]) \times \mathcal{C}^1([0, T] \times X) \times \mathcal{C}([0, T] \times X) \quad (55)$$

$$\mathcal{Y}' = 0 \times \mathcal{M}([-\tau, 0]) \times \mathcal{C}^1([0, T] \times X)' \times \mathcal{M}([0, T] \times X). \quad (56)$$

The space \mathcal{X} has the weak-* topology and \mathcal{Y} has a sup-norm bounded weak topology. Because there are no affine-inequality constraints present in (17b)-(17e), we write $\mathcal{Y}_+ = \mathcal{Y}$ and $\mathcal{Y}'_+ = \mathcal{Y}'$ to match the notation used in [46].

The variables of (18) with $\ell = (\gamma, \xi, v, \phi)$ satisfy $\ell \in \mathcal{Y}'_+$.

A pair of adjoint linear operators $\mathcal{A} : \mathcal{X}_+ \rightarrow \mathcal{Y}_+$ and $\mathcal{A}' : \mathcal{Y}'_+ \rightarrow \mathcal{X}'_+$ induced from (17b)-(17e) are,

$$\mathcal{A}(\boldsymbol{\mu}) = \begin{bmatrix} \langle 1, \mu_0 \rangle \\ \pi_{\#}^t \mu_h \\ \mu_p - \delta_0 \otimes \mu_0 - \mathcal{L}_f^\dagger \mu \\ S_{\#}^\tau (\mu_h + \pi_{\#}^{tx_0} \bar{\mu}_0) - \pi_{\#}^{tx_1} (\bar{\mu}_0 + \bar{\mu}_1) - \nu \end{bmatrix} \quad (57)$$

$$\mathcal{A}'(\boldsymbol{\ell}) = \begin{bmatrix} \xi(t) + \phi(t + \tau, x) \\ \gamma - v(0, x) \\ v(t, x) \\ -\phi(t, x) \\ -\mathcal{L}_f v(t, x_0) - \phi(t, x_1) + \phi(t + \tau, x_0) \\ -\mathcal{L}_f v(t, x_0) - \phi(t, x_1) \end{bmatrix}.$$

The cost and answer vectors are

$$\mathbf{c} = [0, 0, p, 0, 0, 0] \quad (58)$$

$$\mathbf{b} = [1, \lambda_{[-\tau, 0]}, 0, 0]. \quad (59)$$

Problem 17 may be expressed as the standard-form LP:

$$p^* = \sup_{\boldsymbol{\mu} \in \mathcal{X}_+} \langle \mathbf{c}, \boldsymbol{\mu} \rangle = \langle p, \mu_p \rangle, \quad \mathbf{b} - \mathcal{A}(\boldsymbol{\mu}) \in \mathcal{Y}_+. \quad (60)$$

The standard-form dualization of (60) is

$$d^* = \inf_{\boldsymbol{\ell} \in \mathcal{Y}'_+} \langle \boldsymbol{\ell}, \mathbf{b} \rangle = \gamma + \int_{t=-\tau}^0 \xi(t) dt, \quad \mathcal{A}'(\boldsymbol{\ell}) - \mathbf{c} \in \mathcal{X}_+. \quad (61)$$

The standard-form (61) may be expanded into (18).

Given that all sets are compact (A1), measures in $\boldsymbol{\mu}$ are bounded (Lemma 4.2), functions in (c, \mathcal{A}) are continuous (A2, A4, $v \in C^1([0, T] \times X) \implies \mathcal{L}_f v \in C([0, T] \times X)$), and there exists a feasible measure solution (Theorem 3.2); it holds that strong duality between (17) and (18) is achieved by Theorem 2.6 of [46].

C Subvalue Functionals and DDE Control

This appendix analyzes a DDE OCP when posed over a given history $x_h(\cdot)$. The function $J(t, x_0, x_1, u)$ is a running cost evaluated on the trajectory starting from x_h , and $J_T(x)$ is a terminal cost at time T . The final point $x(T)$ must reside in the terminal set $X_T \subseteq X$. The controller $u(\cdot)$ must reside inside the compact set $U \subset \mathbb{R}^m$ at each time. The DDE OCP under these constraints is

$$P^* = \inf_{u(t)} \int_{t=0}^T J(t, x(t), x(t - \tau), u(t)) dt + J_T(x(T)) \quad (62a)$$

$$\dot{x} = f(t, x(t), x(t - \tau), u(t)) \quad \forall t \in [0, T] \quad (62b)$$

$$u(t) \in U \quad \forall t \in [0, T] \quad (62c)$$

$$x(t) = x_h(t) \quad \forall t \in [-\tau, 0] \quad (62d)$$

$$x(T) \in X_T. \quad (62e)$$

Problem 62 was addressed in works such as [7, 10, 12, 11, 47], and was completely solved in the case of linear DDE dynamics and a quadratic objective in [48, 49].

A pair of infinite-dimensional LPs are synthesized to bound the OCP in (62).

This appendix assumes that the terminal time T is fixed to simplify analysis. The MV-solution from Section 3 involves a free terminal time, multiple histories, and zero running cost ($J = 0$).

C.1 Control Measure Program

The deterministic control law $u(t, x_0, x_1)$ at each time t is relaxed into a probability distribution $\xi_u(u \mid t, x_0, x_1)$ [8].

The measures involved in a MV-solution of (62) are

$$\text{Initial} \quad \mu_0 \in \mathcal{M}_+(X_0) \quad (63a)$$

$$\text{Peak} \quad \mu_p \in \mathcal{M}_+([0, T] \times X) \quad (63b)$$

$$\text{Occupation Start} \quad \bar{\mu}_0 \in \mathcal{M}_+([0, \kappa T] \times X^2 \times U) \quad (63c)$$

$$\text{Occupation End} \quad \bar{\mu}_1 \in \mathcal{M}_+([\kappa T, T] \times X^2 \times U). \quad (63d)$$

The time-slack measure is set to $\nu = 0$ because of the fixed-terminal-time setting ($t^* = T$). The symbol $\mu_{x_h(\cdot)}$ is the occupation measure of $t \mapsto (t, x_h(t))$ between $t \in [-\tau, 0]$. The history measure μ_h from (9) is set equal to $\mu_{x_h(\cdot)}$ in the case of a single history. Similarly, the initial measure μ_0 is set to the Dirac delta $\delta_{x=x_h(0^+)}$.

A measure relaxation to the optimal program in (62) is

$$p^* = \inf \quad \langle J, \bar{\mu} \rangle + \langle J_T, \mu_T \rangle \quad (64a)$$

$$\delta_T \otimes \mu_T = \delta_{t=0, x=x_h(0^+)} + \pi_{\#}^{tx_0} \mathcal{L}_f^\dagger(\bar{\mu}_0 + \bar{\mu}_1) \quad (64b)$$

$$\pi_{\#}^{tx_1}(\bar{\mu}_0 + \bar{\mu}_1) = S_{\#}^\tau(\mu_{x_h(\cdot)} + \pi_{\#}^{tx_0} \bar{\mu}_0) \quad (64c)$$

$$\text{Measures from (63)}. \quad (64d)$$

This measure relaxation is based on the optimal control framework of [13, 16]. Young measure formulations for DDE OCP have been developed in [7, 10, 12, 11, 9], but Liouville equations began use only in [27].

C.2 Control Function Program

Dual variables $v \in C^1([0, T] \times X)$ and $\phi \in C([0, T] \times X)$ may be introduced to form the dual program of (64):

$$d^* = \sup \quad v(0, x_h(0)) + \int_{-\tau}^0 \phi(t + \tau, x_h(t)) dt \quad (65a)$$

$$J_T(x) - v(T, x) \geq 0 \quad \forall x \in X_T \quad (65b)$$

$$\mathcal{L}_f v + J(t, x_0, u) - \phi(t, x_1) + \phi(t + \tau, x_0) \geq 0 \quad \forall (t, x_0, x_1, u) \in [0, T - \tau] \times X^2 \times U \quad (65c)$$

$$\mathcal{L}_f v + J(t, x_0, u) - \phi(t, x_1) \geq 0 \quad \forall (t, x_0, x_1, u) \in [T - \tau, T] \times X^2 \times U \quad (65d)$$

$$v \in C^1([0, T] \times X) \quad (65e)$$

$$\phi \in C([0, T] \times X). \quad (65f)$$

This dual program is obtained (with strong duality) by following nearly identical steps to Appendix B.

C.3 True Value Functional

Let \mathcal{U} be the admissible class of control inputs (such as $\mathcal{U} = \{u : [0, T] \rightarrow U\}$). Given a time $t \in [0, T]$, a current state $z \in X$, and a history $w(\cdot) \in PC([-\tau, 0], X)$, the value functional V^* associated with the OCP (62) is

$$\begin{aligned}
V^*(t, z, w(\cdot)) &= \min_{u \in \mathcal{U}} \int_{t' = t}^T J(t', x(t' | t, w, u), u(t')) dt' + J_T(x(T | t, w, u)) \\
\dot{x} &= f(t, x(t), x(t - \tau), u(t)) & \forall t \in [0, T] \\
x(t') &= w(t') & \forall t \in [t - \tau, t] \\
x(t) &= z \\
x(T) &\in X_T \\
u(t) &\in U & \forall t \in [0, T].
\end{aligned} \tag{66}$$

The value functional V^* is the cost of solving Problem (62) starting at time t and state z with history $w(\cdot)$. The convention of arguments $t, z, w(\cdot)$ was taken from [47].

The Hamilton-Jacobi-Bellman (HJB) equation of optimality is [50]

$$0 = J_T(x(T)) - V^*(T, x(T)) \tag{67a}$$

$$0 = \inf_{u \in U} \left(\dot{V}^*(t, x(t), x_\tau(\cdot), u) + J(t, x(t), u(t)) \right) \quad \forall t \in [0, T]. \tag{67b}$$

The Cauchy problem of (7, 8) in [47] has the form of (67).

C.4 Subvalue Functional

The solution of program (65) can create a lower-bound on the value functional V^* .

C.4.1 Properties of Subvalue Functionals

Definition C.1. A subvalue functional is a functional $\mathcal{V}(t, x, w)$ such that

$$\mathcal{V}(t, x, w) \leq V^*(t, x, w) \quad \forall t \in [0, T], x \in X, w \in PC([-\tau, 0], X). \tag{68}$$

Theorem C.1. Any functional $\mathcal{V}(t, x, x_\tau)$ with derivative $\dot{\mathcal{V}}(t, x, x_\tau, u)$ that satisfies the following two properties is a subvalue functional for V^* :

$$J_T(x) - \mathcal{V}(T, x, w) \geq 0 \quad \forall x \in X_T, w \in PC([-\tau, 0], X) \tag{69a}$$

$$J(t, x, u) + \dot{\mathcal{V}}(t, x, w, u) \geq 0, \quad \forall t \in T, x \in X, w \in PC([-\tau, 0], X), u \in U. \tag{69b}$$

Proof. This result follows by following the steps of Proposition 1's proof from [51].

Let $\tilde{u} \in \mathcal{U}$ be an arbitrary control policy starting at the initial condition (t_0, z, w) , resulting in a trajectory $\tilde{x}(t)$. Denote $\tilde{x}_\tau(\cdot)$ as the history function $\tilde{x}_i(t') = \tilde{x}(t + t')$ $\forall t' \in [-\tau, 0]$.

Relation (69b) ensures that for all $t \in [t_0, T]$,

$$\dot{\mathcal{V}}(t, \tilde{x}(t), \tilde{x}_i(\cdot), \tilde{u}(t)) + J(t, \tilde{x}(t), \tilde{u}(t)) \geq 0. \tag{70}$$

Integrating the above term with respect to t yields

$$0 \leq \int_{t=t_0}^T \dot{\mathcal{V}}(t, \tilde{x}(t), \tilde{x}_i(\cdot), \tilde{u}(t)) + J(t, \tilde{x}(t), \tilde{u}(t)) dt \tag{71a}$$

$$0 \leq \underbrace{\mathcal{V}(T, \tilde{x}(T), \tilde{x}_T(\cdot))}_{\mathcal{V}(T)} - \underbrace{\mathcal{V}(t_0, \tilde{x}(t_0), \tilde{x}_{t_0}(\cdot))}_{\mathcal{V}(t_0)} + \int_{t=t_0}^T J(t, \tilde{x}(t), \tilde{u}(t)) dt \tag{71b}$$

$$\mathcal{V}(t_0) \leq \mathcal{V}(T) + \int_{t=t_0}^T J(t, \tilde{x}(t), \tilde{u}(t)) dt \tag{71c}$$

$$\mathcal{V}(t_0) \leq J_T(\tilde{x}(T)) + \int_{t=t_0}^T J(t, \tilde{x}(t), \tilde{u}(t)) dt. \tag{71d}$$

The transformation of (71c) to (71d) follows from relations (73) and (65b) ($\mathcal{V}(T) \leq J(\tilde{x}(T))$). When \tilde{u} is a minimizing control u^* (if it exists), then the right-hand side of (71d) is the optimal value functional $V^*(t_0, z, w(\cdot))$ and the left-hand side is $\mathcal{V}(t_0, z, w(\cdot))$. The proof that \mathcal{V} is a lower bound on V^* is therefore complete, given that $\mathcal{V}(t_0, z, w(\cdot)) \leq V^*(t_0, z, w(\cdot))$ will hold for all choices of $(t_0, z, w(\cdot))$. \square

C.4.2 Recovery of a Subvalue Functional

The dual solution (v, ϕ) from (65) may be assembled into a functional,

$$V(t, x, z(\cdot)) = v(t, x) + \int_t^{\min(t+\tau, T)} \phi(s, z(s-\tau)) ds. \quad (72)$$

The bias term ϕ in (65f) is defined and is C^0 continuous only between times $t \in [0, T]$. If the hard integration limit at T was not present, then ϕ would be queried at undefined values $t \in (T, T + \tau]$. The terminal value of the value functional is

$$V(T) = V(t, x(T), x([T-\tau, T])) = v(T, x(T)) + \int_T^T \phi_i(s, x(s-\tau)) ds = v(T, x(T)). \quad (73)$$

The objective in (65a) is the evaluation of the value functional at time $t = 0$ along the optimal controlled trajectory $x^*(t)$:

$$V(0) = V(0, x_h(0), x_h) = v(0, x_h(0)) + \int_0^\tau \phi_i(s, x_h(s-\tau)) ds. \quad (74)$$

The time-derivative (co-invariant derivative) of the value functional \dot{V} is

$$\dot{V}(t, z, w(\cdot), u) = \mathcal{L}_f v(t, x(t)) + I_{[0, T-\tau]}(t) \phi(t+\tau, z) - \phi(t, w(-\tau)). \quad (75)$$

Theorem C.2. *The functional (72) is a subvalue functional in the sense of (C.1).*

Proof. The terminal constraint (65b) satisfies (69a) given the terminal value evaluation in (73). The combination of (65c) and (65d) together satisfy (69b) under the derivative value expression in (75). \square

C.4.3 Continuity of the Recovered Value Functional

Let $u^*(t) \in \mathcal{U}$ be the optimal (infimizing) trajectory of problem (62) given $z, w(\cdot)$, inducing a controlled trajectory $x^*(t) = x(t \mid z, w(\cdot))$. The value functional evaluated along the optimal trajectory $V^*(t) = V(t, x^*(t), x^*([t-\tau, t])$ is C^0 -continuous in t , but is not necessarily C^1 -continuous in t . At the time $t = T - \tau$, define the value functional evaluations

$$V_-^* = \lim_{t \rightarrow (T-\tau)^-} V^*(t) \quad V_+^* = \lim_{t \rightarrow (T-\tau)^+} V^*(t). \quad (76)$$

The difference in these evaluations for every lag i^* is

$$\Delta V^* = V_-^* - V_+^* = \left(\int_{T-\tau^-}^{T^-} - \int_{T-\tau^+}^{T^+} \right) \phi(s, x(s-\tau_i)) ds = 0. \quad (77)$$

The value functional $V^*(t)$ is therefore a member of $C^0([0, T])$ given that $v \in C^1([0, T] \times X)$ and $\phi \in C^0([0, T] \times X)$.

The value functional derivative evaluations are

$$\dot{V}_-^* = \lim_{t \rightarrow (T-\tau)^-} \dot{V}^*(t) \quad \dot{V}_+^* = \lim_{t \rightarrow (T-\tau)^+} \dot{V}^*(t). \quad (78)$$

The difference in the derivative evaluations on both sides of $t = T - \tau$ is

$$\Delta \dot{V}^* = \dot{V}_-^* - \dot{V}_+^* = \phi(T, x(T-\tau)). \quad (79)$$

It is not guaranteed that $\phi(T, x(T-\tau)) = 0$, so the value functional V^* may have discontinuous first derivatives. The value functional is therefore C^0 in time along trajectories, and fails to be C^1 at the time $t = T - \tau$.

We form an additional conjecture to 3.1 in the OCP case based on the tightness conditions in [13].

Conjecture C.1. *Assume for the purposes of this conjecture that:*

A1' The sets $\{[-\tau, T], X, X_T, U\}$ are all compact.

A2' The costs J, J_T are continuous.

A3' The dynamics $f(t, x_0, x_1, u)$ are Lipschitz in their arguments.

A4' The history x_h is inside $PC([-\tau, 0], X)$.

A5' The image of $f(t, x_0, X, U)$ is convex for each fixed (t, x_0) .

A6' The mapping $v \mapsto \inf_{u \in U} J(t, x_0, x_1, u) : f(t, x_0, x_1, u) = v$ is convex in $v \in \mathbb{R}^n$.

Then there is no relaxation gap between (62) and (65) ($P^ = p^*$).*

C.5 Approximate Recovery

A control policy $u(t)$ may be extracted from the value functional V through the trajectory condition (67b) by

$$u(t) = \operatorname{argmin}_u \mathcal{L}_f v(t, x(t)) + I_{[0, T-\tau]}(t) \phi(t + \tau, x(t)) * -\phi(t, x(t - \tau)) + J(t, x(t), u(t)) \quad (80a)$$

$$= \operatorname{argmin}_u f(t, x(t), x(t - \tau), u) \cdot \nabla_x v(t, x(t)) + J(t, x(t), u). \quad (80b)$$

The work in [51] quantifies performance bounds of polynomial value function approximations for ODE systems in terms of W^1 Sobolev norms away from the true value function. Quantifying performance bounds of the extracted controller of (80a) is an open problem.

C.6 Example of Optimal Control

An example of optimal control is presented on the one-dimensional linear system:

$$\begin{aligned} x'(t) &= -3x(t) - 5x(t - 0.25) + u & \forall t \in [0, 1] \\ x_h(t) &= -1 & \forall t \in [-0.25, 0]. \end{aligned} \quad (81)$$

This system has one lag with $\tau = 0.25$ and a time horizon of $T = 1$. The state and control constraints are $X = [-1, 1]$ and $U = [-1, 1]$. With a control weight of $R = 0.01$, the penalties are

$$J(t, x, u) = 0.5x^2 + 0.5Ru^2 \quad J_T(x) = 0. \quad (82)$$

The open loop total cost is 0.0674. Table 2 lists optimal control value approximations for this system.

Table 2: SDP approximation bounds to program (64)

order	1	2	3	4	5	6
bound	7.90E-05	0.0322	0.0386	0.0391	0.0393	0.0393

The applied control $u(t)$ may be recovered through equation (80a) as

$$u(t) = \operatorname{Saturate}_{[-1, 1]} \left(-\frac{1}{R} \partial_x v(t, x(t)) \right). \quad (83)$$

The trajectories and nonnegative functions are plotted for order 4 in Figures 13-14. The order 4 control bound is 0.0391, and the cost evaluated along the controlled trajectory is 0.0394.

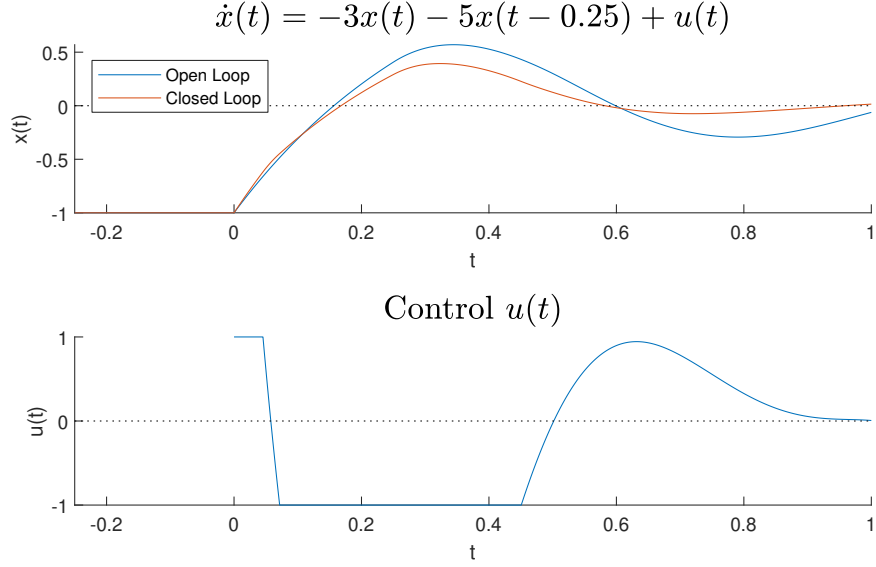


Figure 13: Open and closed loop trajectory with control

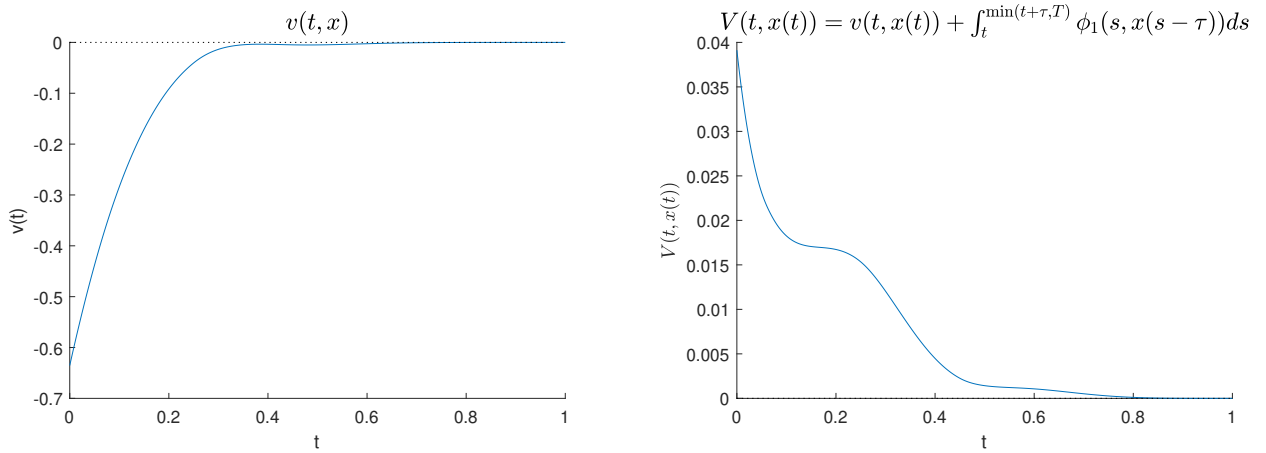


Figure 14: Auxiliary function v and value functional V from (72)

D Improved Accuracy of Control Problems

This appendix lays out methods to reduce the conservatism of DDE OCPs from appendix C by adding new infinite-dimensional nonnegativity constraints.

All approaches discussed in this appendix may be applied to peak estimation, but are presented here in the simplified fixed-terminal-time single-history OCP setting.

D.1 Spatial Partitioning

The constraints (65b)-(65d) must hold in support sets defined by $[0, T] \times X \times U$. Assume that there exists a decomposition of the state spaces $X = \cup_k X_k$ such that $\forall k : \dim(X_k) = n$ and $\forall k, k' : \text{int}(X_k \cap X_{k'}) = \emptyset$ (cells X_k are full-dimensional and their intersections are not full dimensional). Further assume a similar decomposition exists for the control set $U = \cup_\ell U_\ell$.

Let $(v_k(t, x), \phi_k(t, x))$ be functions associated with each space X^k . A space-control partition of (65) is:

$$d^* = \sup \sum_k (I_{X_k}(x_h(0))v_k(0, x_h(0))) + \int_{-\tau}^0 \phi(t + \tau, x_h(t))dt \quad (84a)$$

$$\forall x \in X_k :$$

$$J_T(x) - v_k(T, x) \geq 0 \quad (84b)$$

$$\forall(t, x_0, x_1, u) \in [0, T - \tau]X_k \times X_{k'} \times U_\ell :$$

$$\mathcal{L}_f v_k + J(t, x_0, u) - \phi_{k'}(t, x_1) + \phi_k(t + \tau, x_0) \geq 0 \quad (84c)$$

$$\forall(t, x_0, x_1, u) \in [T - \tau, T] \times X_k \times X_{k'} \times U_\ell :$$

$$\mathcal{L}_f v_k + J(t, x_0, u) - \phi_{k'}(t, x_1) \geq 0 \quad (84d)$$

$$\forall(t, x) \in [0, T] \times (X_k \cap X_{k'}) :$$

$$v_k(t, x) = v_{k'}(t, x) \quad (84e)$$

$$\forall k : v_k \in C^1([0, T] \times X_k) \quad (84f)$$

$$\forall k : \phi_k \in C([0, T] \times X_k). \quad (84g)$$

The v_k terms agree on boundary regions between state cells by (84e). The ϕ_k terms remain continuous (bounded measurable), but this partitioning has an impact when evaluating the finite-degree SDPs.

D.2 Temporal Partitioning

We utilize the following lemma to provide conditions for temporal partitioning:

Lemma D.1. *A sufficient condition for $\int_{t_0}^{t_1} g_1(t)dt \geq \int_{t_0}^{t_1} g_2(t)dt$ is that*

$$\forall t \in [t_0, t_1] : g_1(t) \geq g_2(t). \quad (85)$$

Define the following time breaks (partition) arranged in sorted order as

$$T_{break} = \{0, t_1, \dots, t_{k-1}, t_k = T - \tau, t_{k+1}, \dots, t_{k+l-1}, t_{k+l} = T\}. \quad (86)$$

Let $[t_b, t_{b+1}]$ and $[t_{b-1}, t_b]$ be regions in T_{break} . The subvalue functionals from (72) defined in this region must satisfy

$$V_b(t_b, x, z(\cdot)) \geq V_{b-1}(t_b, x, z(\cdot)) \quad (87a)$$

$$v_b(t_b, x) + \int_{t_b}^{\min(t_b + \tau, T)} \phi_b(s, z(s - \tau))ds \geq v_{b-1}(t_b, x) + \int_{t_b}^{\min(t_b + \tau, T)} \phi_{b-1}(s, z(s - \tau))ds. \quad (87b)$$

The sufficient condition in Lemma D.1 may be used to accomplish this relation in (87), ensuring that the subvalue function will always decrease when traversing a time break:

$$v_b(t_b, x) \geq v_{b-1}(t_b, x) \quad \forall x \in X \quad (88a)$$

$$\phi_b(t, x) \geq \phi_{b-1}(t, x) \quad \forall(t, x) \in [t_b, \min(t_b + \tau, T)] \times X. \quad (88b)$$

The resultant time-partitioned LP is,

$$d^* = \sup v(0, x_h(0)) + \int_{-\tau}^0 \phi_{k+\ell}(t + \tau, x_h(t)) dt \quad (89a)$$

$$\forall x \in X :$$

$$J_T(x) - v_{k+\ell}(T, x) \geq 0 \quad (89b)$$

$$\forall (t, x_0, x_1, u) \in [t_{k'}, t_{k'+1}] \times X^2 \times U, k' = 0..k-1 :$$

$$\mathcal{L}_f v_{k'} + J(t, x_0, u) - \phi_{k'}(t, x_1) + \phi_{k'}(t + \tau, x_0) \geq 0 \quad (89c)$$

$$\forall (t, x_0, x_1, u) \in [t_{k'}, t_{k'+1}] \times X^2 \times U, k' = k..k + \ell :$$

$$\mathcal{L}_f v_{k'} + J(t, x_0, u) - \phi_{k'}(t, x_1) \geq 0 \quad (89d)$$

$$\forall x \in X, k' = 1..k + \ell - 1 :$$

$$v_{k'}(t_{k'}, x) \leq v_{k'+1}(t_{k'}, x) \quad (89e)$$

$$\forall (t, x) \in [t_{k'}, \min(t_{k'} + \tau, T)] \times X, k' = 1..k + \ell - 1$$

$$\phi_{k'}(t, x) \leq \phi_{k'+1}(t, x) \quad (89f)$$

$$\forall k' = 0..k + \ell : \quad (89g)$$

$$v_{k'} \in C^1([t_{k'}, t_{k'+1}] \times X) \quad (89h)$$

$$\phi_{k'} \in C([t_{k'}, \min(t_{k'+1} + \tau, T)] \times X). \quad (89i)$$

D.3 Double Integral Functionals

The subvalue functional in (72) has a single integral term for each delay. Some Lyapunov-Krasovskii or Barrier methods for DDE analysis employ double integrals, such as the following functional for a single delay τ [22],

$$\begin{aligned} V(t, z, w) = & v(t, z) + \int_t^{\min(t+\tau, T)} \phi_i(s, w(s - \tau - t)) ds \\ & + \int_t^{\min(t+\tau, T)} \int_{-\tau}^0 \psi(s, q, w(s - \tau - t), w(q)) dq ds. \end{aligned} \quad (90)$$

The time derivative of (90) in the time span $t \in [0, T - \tau]$ is

$$\begin{aligned} \dot{V}(t, z, w) = & \mathcal{L}_f v(t, z) + \phi(t + \tau, w(0)) - \phi(t, w(-\tau)) \\ & + \int_{-\tau}^0 \psi(t + \tau, q, w(0), w(q)) dq \end{aligned} \quad (91)$$

$$- \int_{-\tau}^0 \psi(t, q, w(-\tau), w(q)) dq, \quad (92)$$

and between $t \in (T - \tau, 0]$ is

$$\dot{V}(t, z, w) = \mathcal{L}_f v(t, z) - \phi(t, w(-\tau)) - \int_{-\tau}^0 \psi(t, q, w(-\tau), w(q)) dq. \quad (93)$$

The derivative \dot{V} has a discontinuity present at $t = T - \tau$, just as described in Section (C.4.3).

A sufficient condition for the inequality (69b) to be fulfilled is that the following functions associated with (92) and (93) (moving all terms under the dq integral) are nonnegative:

$$\begin{aligned} \forall t \in [0, T - \tau], (x_0, x_1, \tilde{x}) \in X^3, q \in [-\tau, 0] : \\ \tau^{-1} (\mathcal{L}_f v(t, z) + J(t, x_0, u) + \phi(t + \tau, x_0) - \phi(t, x_1)) \\ + \psi(t + \tau, q, x_0, \tilde{x}) - \psi(t, q, x_0, \tilde{x}) \geq 0 \end{aligned} \quad (94)$$

$$\begin{aligned} \forall t \in [T - \tau, T], (x_0, x_1, \tilde{x}) \in X^3, q : \\ \tau^{-1} (\mathcal{L}_f v(t, z) + J(t, x_0, u) - \phi(t, x_1)) - \psi(t, q, x_0, \tilde{x}) \geq 0. \end{aligned} \quad (95)$$

Lemma D.1 is utilized to enforce nonnegativity of the integral terms in (92) and (93). The τ^{-1} scale factor arises from placing a q -independent term (such as $J(t, x_0, u)$) inside the integral. The variable $q \in [-\tau, 0]$

is the integrated (swept) time, and $\tilde{x} \in X$ abstracts out the swept state $w(q)$. The dual formulation of constraints (94) and (95) involve occupation measures $\bar{\mu}_0 \in \mathcal{M}_+([0, T - \tau] \times X^3 \times U)$ and $\bar{\mu}_1 \in \mathcal{M}_+([T - \tau, T] \times X^3 \times U)$. This construction may be generalized to DDEs with r delays by adding a double-integral term for each delay.

E Joint+Component Measure

This appendix details an alternate notion of MV-solutions for DDEs. Solving peak estimation problems through these methods will return more conservative but quicker-executing programs (computationally) as compared to the results in Section 3.

E.1 Measure Program

The MV-solution involves a joint occupation measure $\bar{\mu}$ and component measures ω_0, ω_1 :

$$\text{History} \quad \mu_h \in \mathcal{M}_+(H_0) \quad (96a)$$

$$\text{Initial} \quad \mu_0 \in \mathcal{M}_+(X_0) \quad (96b)$$

$$\text{Peak} \quad \mu_p \in \mathcal{M}_+([0, T] \times X) \quad (96c)$$

$$\text{Time-Slack} \quad \nu \in \mathcal{M}_+([0, T] \times X) \quad (96d)$$

$$\text{Joint Occupation} \quad \bar{\mu} \in \mathcal{M}_+([0, T] \times X^2) \quad (96e)$$

$$\text{Component Start} \quad \omega_0 \in \mathcal{M}_+([0, T - \tau] \times X) \quad (96f)$$

$$\text{Component End} \quad \omega_1 \in \mathcal{M}_+([T - \tau, T] \times X). \quad (96g)$$

The peak estimation LP for the Joint+Component framework is

$$p^* = \sup \langle p, \mu_p \rangle \quad (97a)$$

$$\langle 1, \mu_0 \rangle = 1 \quad (97b)$$

$$\pi_{\#}^t \mu_h = \lambda_{[-\tau, 0]} \quad (97c)$$

$$\mu_p = \delta_0 \otimes \mu_0 + \pi_{\#}^{tx_0} \mathcal{L}_f^\dagger \bar{\mu} \quad (97d)$$

$$\pi_{\#}^{tx_0} \bar{\mu} = \omega_0 + \omega_1 \quad (97e)$$

$$\pi_{\#}^{tx_1} \bar{\mu} + \nu = S_{\#}^\tau(\mu_h + \omega_0) \quad (97f)$$

$$\text{Measure Definitions from (96)}. \quad (97g)$$

The history-validity and Liouville constraints in (97) are the same as in (17) under the relation $\bar{\mu} = \bar{\mu}_0 + \bar{\mu}_1$. The consistency constraint in the Joint+Component formulation is split up into the pair (97e)-(97f).

Theorem E.1. *Program (97) returns an upper bound on (1).*

Proof. Let $x_h \in \mathcal{H}$ be a history that generates the trajectory $x(t | x_h)$, and let $t^* \in [0, T]$ be a stopping time.

Just as in Theorem 3.2, measures can be picked as $\mu_0 = \delta_{x=x_h(0+|x_h)}$, $\mu_p = \delta_{t=t^*} \otimes \delta_{x=x(t^*|x_h)}$, μ_h as the occupation measure of $x_\xi(t)$ in the times $[-\tau, 0]$, and $\bar{\mu}$ as the occupation measure of $z(t) = (x(t | x_h), x(t - \tau | x_h))$ in the times $[0, t^*]$.

When $t^* \in [0, T - \tau]$, then ω_0 is the occupation measure of $x(t | x_h)$ in times $[0, t^*]$, ω_1 is the zero measure, and ν is the occupation measure of $x(t - \tau | x_h)$ in times $[t^*, t^* + \tau]$. When $t^* \in (T - \tau, T]$, then ω_0 is the occupation measure of $x(t | x_h)$ in the times $[0, T - \tau]$, ω_1 is the occupation measure of $x(t | x_h)$ in the times $[T - \tau, t^*]$, and ν is the occupation measure of $x(t - \tau | x_h)$ in the times $[T - \tau, T]$.

All measures inside (96) have been defined for a valid trajectory, proving that (97) upper-bounds (1). \square

Theorem E.2. *The Joint+Component measure program (97) is also an upper bound on (17).*

Proof. Let $(\mu_h, \mu_0, \mu_p, \nu, \bar{\mu}_0, \bar{\mu}_1)$ be a feasible set of measures for the constraints of (17).

After performing the following definitions,

$$\bar{\mu} = \bar{\mu}_0 + \bar{\mu}_1 \quad \omega_0 = \pi^{tx_0} \bar{\mu}_0 \quad \omega_1 = \pi^{tx_0} \bar{\mu}_1, \quad (98)$$

the measures $(\mu_h, \mu_0, \mu_p, \nu, \bar{\mu}, \omega_0, \omega_1)$ are feasible solutions for the constraints of (97). \square

Note how the Joint+Component MV-solution involves only one measure involving (t, x_0, x_1) together ($\bar{\mu}$ in (96d)), while the solution in (9) has two measures ($\bar{\mu}_0, \bar{\mu}_1$). Application of the moment-SOS hierarchy towards solving problems in (96d) result in only one Gram matrix of maximal size $\binom{1+2n+d}{d}$.

E.2 Function Program

The gap between (97) and (17) can most easily be observed by examining the dual program of (97):

$$d^* = \inf_{\gamma \in \mathbb{R}} \gamma + \int_{t=-\tau}^0 \xi(t) dt \quad (99a)$$

$$\gamma \geq v(0, x) \quad \forall x \in X_0 \quad (99b)$$

$$v(t, x) \geq p(x) \quad \forall (t, x) \in [0, T] \times X \quad (99c)$$

$$\xi(t) + \phi_1(t + \tau, x) \quad \forall (t, x) \in H_0 \quad (99d)$$

$$0 \geq \mathcal{L}_f v(t, x_0) + \phi_0(t, x_0) + \phi_1(t, x_1) \quad \forall (t, x_0, x_1) \in [0, T] \times X^2 \quad (99e)$$

$$\phi_1(t, x) \leq 0 \quad \forall (t, x) \in [0, T] \quad (99f)$$

$$\phi_0(t, x) + \phi_1(t + \tau, x) \geq 0 \quad \forall (t, x) \in [0, T - \tau] \times X \quad (99g)$$

$$\phi_0(t, x) \geq 0 \quad \forall (t, x) \in [T - \tau, T] \times X \quad (99h)$$

$$v(t, x) \in C^1([0, T] \times X) \quad (99i)$$

$$\phi_0(t, x), \phi_1(t, x) \in C([0, T] \times X) \quad (99j)$$

$$\xi(t) \in C([-\tau, 0]). \quad (99k)$$

Adding together (99e) and (99g) yields constraint (18f) in $[0, T - \tau] \times X^2$. Similarly, the addition of (99e) and (99h) forms constraint (18g). The dual formulation in (99) enforces nonnegativity of addends inside whole-terms of (17). The constraints of (99) are stricter than of (18), resulting in a lowered infimum/upper bound on peak value.

E.3 Joint+Component Example

Table (3) compares moment-SOS SDPs associated to programs (17) and (97) for the delayed Flow example in Section 5.2.

Table 3: Comparison of (17) and (97) SDP bounds for the delayed Flow system

degree d	1	2	3	4	5
Joint+Component (97)	1.25	1.223	1.1937	1.1751	1.1636
Standard (17)	1.25	1.2183	1.1913	1.1727	1.1630

Table 4: Time (seconds) to obtain SDP bounds in Table 3

degree d	1	2	3	4	5
Joint+Component (97)	0.782	0.991	5.271	31.885	336.509
Standard (17)	0.937	1.190	9.508	105.777	552.496